A Bioconductor workflow for the Bayesian analysis of spatial proteomics

true
true
true
true
true

Abstract

Knowledge of the subcellular location of a protein gives valuable insight into its function. The field of spatial proteomics has become increasingly popular due to improved multiplexing capabilities in high-throughput mass spectrometry, which have made it possible to systematically localise thousands of proteins per experiment. In parallel with these experimental advances, improved methods for analysing spatial proteomics data have also been developed. In this workflow, we demonstrate using `pRoloc` to perform Bayesian analysis of spatial proteomics data. We detail the software infrastructure and then provide step-by-step guidance of the analysis, including setting up a pipeline, assessing convergence, and interpreting downstream results. In several places we provide additional details on Bayesian analysis to provide users with a holistic view of Bayesian analysis for spatial proteomics data.

R version: R version 3.5.2 (2018-12-20)

Bioconductor version: 3.8

Introduction

Determining the spatial subcellular distribution of proteins enables novel insight into protein function (Crook et al. 2018). Many proteins function within a single location within the cell; however, it is estimated that up to half of the proteome is thought to reside in multiple locations, with some of these undergoing dynamic relocalisation (Thul et al. 2017). These phenomena lead to variability and uncertainty in robustly assigning proteins to a unique localisation. Functional compartmentalisation of proteins allows the cell to control biomolecular pathways and biochemical processes within the cell. Therefore, proteins with multiple localisations may have multiple functional roles (Jeffery 2009). Machine learning algorithms that fail to quantify uncertainty are unable to draw deeper insight into understanding cell biology from mass spectrometry (MS)-based spatial proteomics experiments. Hence, quantifying uncertainty allows us to make rigorous assessments of protein subcellular localisation and multi-localisation.

For proteins to carry out their functional role they must be localised to the correct subcellular compartment, ensuring the biochemical conditions for desired molecular interactions are met (Gibson 2009). Many pathologies, including cancer and obesity are characterised by protein mis-localisations (Olkkonen and Ikonen 2006; Laurila and Vihinen 2009; Luheshi, Crowther, and Dobson 2008; De Matteis and Luini 2011; Cody, Iampietro, and Lécuyer 2013; Kau, Way, and Silver 2004; Rodriguez, Au, and Henderson 2004; Latorre et al. 2005; Shin et al. 2013; Siljee et al. 2018). High-throughput spatial proteomics technologies have seen rapid improvement over the last decade and now a single experiment can provide spatial information on thousands of proteins at once (Dunkley et al. 2006; Foster et al. 2006; Christoforou et al. 2016; Geladaki et al. 2019). As a result of these spatial proteomics technologies many biological systems have been characterised (Dunkley et al. 2006; Tan et al. 2009; Hall et al. 2009; Breckels et al. 2013; Christoforou et al. 2016; Thul et al. 2017). The popularity of such methods is now evident with many new studies in recent years (Christoforou et al. 2016; Beltran, Mathias, and Cristea 2016; Jadot et al. 2017; Itzhak et al. 2017; Mendes et al. 2017; Hirst et al. 2018; Davies et al. 2018; Orre et al. 2019; Nightingale et al. 2019).

Mass spectrometry-based spatial proteomic experiments begin with the gentle lysis of a population of cells in a fashion that maintains the integrity of the organelles. To separate cellular content a variety of methods are available, including equilibrium gradient-density separation (Christoforou et al. 2016; Mulvey et al. 2017) or differential centrifugation (Geladaki et al. 2019). For example, in hyperLOPIT (Mulvey et al. 2017) cell lysis is followed by the separation of subcellular components along a continuous density gradient based on their buoyant density. Discrete fractions along this gradient are then collected, and protein distributions revealing organelle specific correlation profiles within the fractions are achieved using high accuracy MS. Proteins from the dataset are then manually annotated with well-documented single localisations curated from the literature, referred to as organelle markers (see Gatto et al. (Gatto, Breckels, et al. 2014a)). A prediction model is then trained from these markers to create a classifier, which assigns proteins with unknown localisation to a sub-cellular niche (Gatto, Breckels, et al. 2014a).

Bayesian approaches to machine learning and statistics can provide more insight, by providing uncertainty quantification (Gelman et al. 1995). In a parametric Bayesian setting, a parametric model is proposed, along with a statement about our prior beliefs of the model parameters. Bayes' theorem tells us how to update the prior distribution of the parameters to obtain the posterior distribution of the parameters after observing the data. It is the posterior distribution which quantifies the uncertainty in the parameters. This contrasts from a maximum-likelihood approach where we obtain only a point estimate of the parameters.

Adopting a Bayesian framework for data analysis, though of much interest to experimentalists, can be challenging. Once we have specified a probabilistic model, computational approaches are typically used to obtain the posterior distribution upon observation of the data. These algorithms can have parameters that require tuning and a variety of settings, hindering their practical use by those not familiar with Bayesian methodology. Even once the algorithms have been correctly set-up, assessments of convergence and guidance on how to interpret the results are often sparse. This workflow presents a Bayesian analysis of spatial proteomics to elucidate the process for practitioners. Our workflow also provides a template for others interested in designing tools for the biological community which rely on Bayesian inference.

Our model for the data is the t-augmented Gaussian mixture (TAGM) model proposed in (Crook et al. 2018). Crook et al. (2018) provide a detailed description of the model, rigorous comparisons and testing on many spatial proteomics datasets. In addition, they include a case study of a hyperLOPIT experiment performed on mouse pluripotent stem cells (Christoforou et al. 2016; Mulvey et al. 2017). Revisiting these details is not the purpose of this computational protocol; rather we present how to correctly use the software and provide step-by-step guidance for interpreting the results.

In brief, the TAGM model posits that each annotated sub-cellular niche can be modelled using a Gaussian distribution. Thus the full complement of proteins within the cell is captured as a mixture of Gaussians. The highly dynamic nature of the cell means that many proteins are not well captured by any of these multivariate Gaussian distributions, and thus the model also includes an outlier component, which is mathematically described as a multivariate student's t distribution. The heavy tails of the t distribution allow it to better capture dispersed proteins. The outlier component is included to avoid allocating proteins which are far from any annotated subcellular niche. These proteins can be interpreted in multiple ways: they could be part of an unannotated subcellular niche, they could reside in multiple locations, they could have highly variable sub-cellular niches or they could have been poorly quantified.

There are two approaches to perform inference in the TAGM model. The first, which we refer to as TAGM MAP, allows us to obtain *maximum a posteriori* estimates of posterior localisation probabilities; that is, the modal posterior probability that a protein localises to that class. This approach uses the expectation-maximisation (EM) algorithm to perform inference (Dempster, Laird, and Rubin 1977). Whilst this is an interpretable summary of the TAGM model, it only provides point estimates. For a richer analysis, we also present a Markov-chain Monte-Carlo (MCMC) method to perform fully Bayesian inference in our model, allowing us to obtain full posterior localisation distributions. This method is referred to as TAGM MCMC throughout the text.

This workflow begins with a brief review of some of the basic features of mass spectrometry-based spatial proteomics data, including our state-of-the-art computational infrastructure and bespoke software suite. We then present each method in turn, detailing how to obtain high quality results. We provide an extended

discussion of the TAGM MCMC method to highlight some of the challenges that may arise when applying this method. This includes how to assess convergence of MCMC methods, as well as methods for manipulating the output. We then take the processed output and explain how to interpret the results, as well as providing some tools for visualisation. We conclude with some remarks and directions for the future. Source code for this workflow, including code used to generate tables and figures, is available on GitHub (Oliver M. Crook et al. 2019)

Getting started and infrastructure

In this workflow, we are using version 1.23.2 of `pRoloc` (Gatto, Breckels, et al. 2014b). The package `pRoloc` contains algorithms and methods for analysing spatial proteomics data, building on the `MSnSet` structure provided in `MSnbase`. The `pRolocdata` package provides many annotated datasets from a variety of species and experimental procedures. The following code chunks install and load the suite of packages require for the analysis.

```
if (!require("BiocManager"))
    install.package("BiocManager")
BiocManager::install(c("pRoloc", "pRolocdata"))
```

```
library("pRoloc")
```

```
##
## This is pRoloc version 1.23.2
##   Visit https://lgatto.github.io/pRoloc/ to get started.
```

```
library("pRolocdata")
```

```
##
## This is pRolocdata version 1.21.1.
## Use 'pRolocdata()' to list available data sets.
```

We assume that we have an MS-based spatial proteomics dataset contained in a `MSnSet` structure. For information on how to import data, perform basic data processing, quality control, supervised machine learning and transfer learning we refer the reader to (Breckels, Mulvey, et al. 2016). Here, we start by loading a spatial proteomics dataset on mouse E14TG2a embryonic stem cells (Breckels, Holden, et al. 2016). The LOPIT protocol (Dunkley et al. 2004; Dunkley et al. 2006) was used and the normalised intensity of proteins from eight iTRAQ 8-plex labelled fraction are provided. The methods provided here are independent of labelling procedure, fractionation process or workflow. Examples of valid experimental protocols are LOPIT (Dunkley et al. 2004), hyperLOPIT (Christoforou et al. 2016; Mulvey et al. 2017), label-free methods such as PCP (Foster et al. 2006), and when fractionation is performed by differential centrifugation (Itzhak et al. 2016; Geladaki et al. 2019).

In the code chunk below, we load the aforementioned dataset. The printout demonstrates that this experiment quantified 2031 proteins over 8 fractions.

```
data("E14TG2aR") # load experimental data
E14TG2aR
```

```
## MSnSet (storageMode: lockedEnvironment)
## assayData: 2031 features, 8 samples
##   element names: exprs
## protocolData: none
## phenoData
##   sampleNames: n113 n114 ... n121 (8 total)
##   varLabels: Fraction.information
##   varMetadata: labelDescription
```

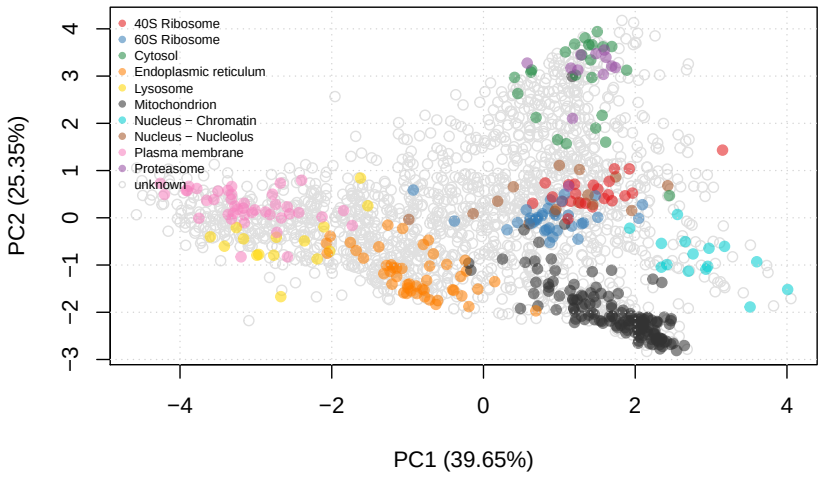

Figure 1: The first two principal component of a mouse embryonic stem cell dataset [@Breckels:2016]. Each pointer represents a protein and marker proteins are coloured according to their localisation. Proteins with unknown localisation are coloured grey.

```
## featureData
##   featureNames: Q62261 Q9JHU4 ... Q9EQ93 (2031 total)
##   fvarLabels: Uniprot.ID UniprotName ... markers (8 total)
##   fvarMetadata: labelDescription
## experimentData: use 'experimentData(object)'
## Annotation:
## - - - Processing information - - -
## Loaded on Thu Jul 16 15:02:29 2015.
## Normalised to sum of intensities.
## Added markers from  'mrk' marker vector. Thu Jul 16 15:02:29 2015
##  MSnbase version: 1.17.12
```

In figure @ref(fig:e14pca1), we can visualise the mouse stem cell dataset using the `plot2D` function. We observe that some of the organelle classes overlap and this is a typical feature of biological datasets. Thus, it is vital to perform uncertainty quantification when analysing biological data.

```
plot2D(E14TG2aR)
addLegend(E14TG2aR, where = "topleft", cex = 0.6)
```

Methods: *TAGM MAP*

Introduction to TAGM MAP

We can use *maximum a posteriori* (MAP) estimation to perform Bayesian parameter estimation for our model. The *maximum a posteriori* estimate is the mode of the posterior distribution and can be used to provide a point estimate summary of the posterior localisation probabilities. In contrast to TAGM MCMC (see later), it does not provide samples from the posterior distribution, however it allows faster inference by using an extended version of the expectation-maximisation (EM) algorithm. The EM algorithm iterates

between an expectation step and a maximisation step. This allows us to find parameters which maximise the logarithm of the posterior density, in the presence of latent (unobserved) variables. The EM algorithm is guaranteed to converge to a local mode. The code chunk below executes the `tagmMapTrain` function for a default of 100 iterations. We use the default priors for simplicity and convenience, however they can be changed, which we explain in a later section. The output is an object of class `MAPParams`, that captures the details of the TAGM MAP model.

```
set.seed(2)
mappars <- tagmMapTrain(E14TG2aR)
```

```
## co-linearity detected; a small multiple of
##               the identity was added to the covariance
```

```
mappars
```

```
## Object of class "MAPParams"
##  Method: MAP
```

Aside: collinearity

The previous code chunk outputs a message concerning data collinearity. This is because the covariance matrix of the data has become ill-conditioned and as a result the inversion of this matrix becomes unstable with floating point arithmetic. This can lead to the failure of standard matrix algorithms upon which our method depends. In this case, it is standard practice to add a small multiple of the identity to stabilise this matrix. The printed message is a statement that this operation has been performed for these data.

Model visualisation

The results of the modelling can be visualised with the `plotEllipse` function on figure @ref(fig:e14ellipse). The outer ellipse contains 99% of the total probability whilst the middle and inner ellipses contain 95% and 90% of the probability respectively. The centres of the clusters are represented by black circumpunct (circled dot). We can also plot the model in other principal components. The code chunk below plots the probability ellipses along the first and second, as well as the fourth principal component. The user can change the components visualised by altering the `dims` argument.

```
par(mfrow = c(2, 1))
plotEllipse(E14TG2aR, mappars)
plotEllipse(E14TG2aR, mappars, dims = c(1, 4))
```

The expectation-maximisation algorithm

The EM algorithm is iterative; that is, the algorithm iterates between an expectation step and a maximisation step until the value of the log-posterior does not change (Dempster, Laird, and Rubin 1977). This fact can be used to assess the convergence of the EM algorithm. The value of the log-posterior at each iteration can be accessed with the `logPosteriors` function on the `MAPParams` object. The code chunk below plots the log posterior at each iteration and we see on figure @ref(fig:mapconverge) the algorithm rapidly plateaus and so we have achieved convergence. If convergence has not been reached during this time, we suggest to increase the number of iterations by changing the parameter `numIter` in the `tagmMapTrain` method. In practice, it is not unexpected to observe small fluctuations due to numerical errors and this should not concern users.

```
plot(logPosteriors(mappars), type = "b", col = "blue",
     cex = 0.3, ylab = "log-posterior", xlab = "iteration")
```

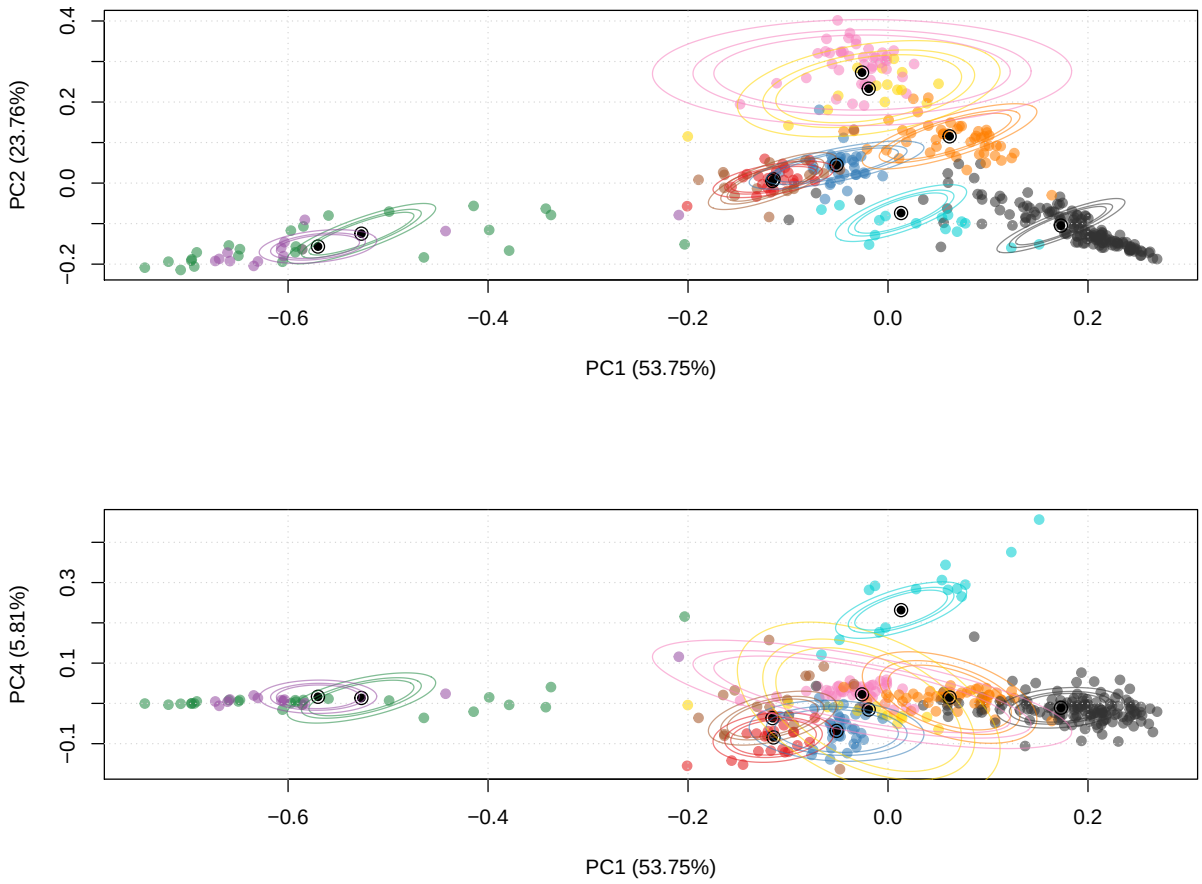

Figure 2: PCA plot with probability ellipses along PC 1 and 2 (left) and PC 1 and 4 (right). The ellipses show the component-conditional densities obtained from the fitted model evaluated at $heta_{extMAP}$

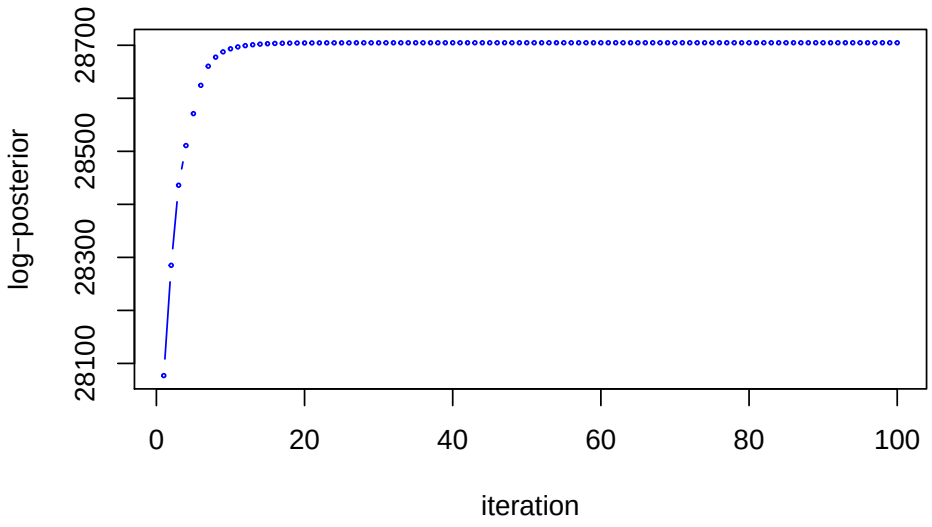

Figure 3: Log-posterior at each iteration of the EM algorithm demonstrating convergence.

The code chunk below uses the `mappars` object generated above, along with the `E14RG2aR` dataset, to classify the proteins of unknown localisation using `tagmPredict` function. The results of running `tagmPredict` are appended to the `fData` columns of the `MSnSet`.

```
E14TG2aR <- tagmPredict(E14TG2aR, mappars) # Predict protein localisation
```

The new feature variables that are generated are:

- `tagm.map.allocation`: the TAGM MAP predictions for the most probable protein sub-cellular allocation.

```
table(fData(E14TG2aR)$tagm.map.allocation)
```

```
##
##          40S Ribosome          60S Ribosome                Cytosol
##                    34                    85                   328
## Endoplasmic reticulum              Lysosome         Mitochondrion
##                   284                   147                   341
##   Nucleus - Chromatin   Nucleus - Nucleolus       Plasma membrane
##                   143                   322                   326
##            Proteasome
##                    21
```

- `tagm.map.probability`: the posterior probability for the protein sub-cellular allocations.

```
summary(fData(E14TG2aR)$tagm.map.probability)
```

```
##    Min. 1st Qu.  Median    Mean 3rd Qu.    Max.
## 0.00000 0.06963 0.93943 0.63829 0.99934 1.00000
```

- `tagm.map.outlier`: the posterior probability for that protein to belong to the outlier component rather than any annotated component.

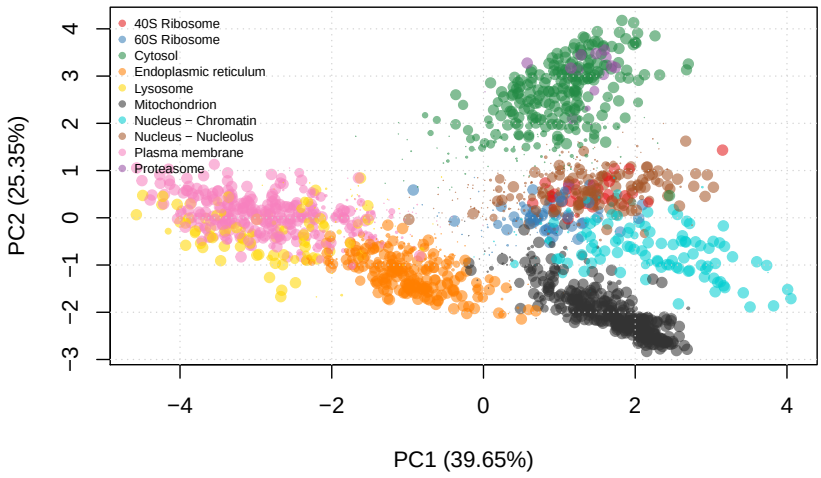

Figure 4: TAGM MAP allocations, where the pointer is scaled according to the localisation probability and coloured according to the most probable subcellular niche.

```
summary(fData(E14TG2aR)$tagm.map.outlier)
```

```
##       Min.    1st Qu.     Median       Mean    3rd Qu.       Max.
## 0.0000000 0.0002363 0.0305487 0.3452624 0.9249810 1.0000000
```

We can visualise the results by scaling the pointer according the posterior localisation probabilities. To do this we extract the MAP localisation probabilities from the feature columns of the the `MSnSet` and pass these to the `plot2D` function (figure @ref(fig:mappca)).

```
ptsze <- fData(E14TG2aR)$tagm.map.probability # Scale pointer size
plot2D(E14TG2aR, fcol = "tagm.map.allocation", cex = ptsze)
addLegend(E14TG2aR, where = "topleft", cex = 0.6, fcol = "tagm.map.allocation")
```

The TAGM MAP method is easy to use and it is simple to check convergence, however it is limited in that it can only provide point estimates of the posterior localisation distributions. To obtain the full posterior distributions and therefore a rich analysis of the data, we use Markov-Chain Monte-Carlo methods. In our particular case, we use a *collapsed Gibbs sampler* (Smith and Roberts 1993).

Methods: *TAGM MCMC* a brief overview

The TAGM MCMC method allows a fully Bayesian analysis of spatial proteomics datasets. It employs a collapsed Gibbs sampler to sample from the posterior distribution of localisation probablities, providing a rich analysis of the data. This section demonstrates the advantage of taking a Bayesian approach and the biological information that can be extracted from this analysis.

For those unfamiliar with Bayesian methodology, some of the key ideas for a more complete understanding are as follows. Firstly, MCMC based inference contrasts with MAP based inference in that it *samples* from the posterior distribution of localisation probabilities. Hence, we do not just have a single estimate for each quantity but a distribution of estimates. MCMC methods are a large class of algorithms used to sample from a probability distribution, in our case the posterior distribution of the parameters (Gilks, Richardson, and

Spiegelhalter 1995). Once we have sampled from the posterior distribution, we can estimate the mean of the posterior distribution by simply taking the mean of the samples. In a similar fashion, we can obtain estimates of other summaries of the posterior distribution.

A schematic of MCMC sampling is provided in figure @ref(fig:mcmcCartoon) to aid understanding. Proteins, coloured blue, are visualised along two variables of the data. Probability ellipses representing contours of a probability distribution matching the distribution of the proteins are overlaid. We now wish to obtain samples from this distribution. The MCMC algorithm is initialised with a starting location, then at each iteration a new value is proposed. These proposed values are either accepted or rejected (according to a carefully computed acceptance probability) and over many iterations the algorithm converges and produces samples from the desired distribution. Samples from this distribution are coloured in red in the schematic figure. A large portion of the earlier samples may not reflect the true distribution, because the MCMC sampler has yet to converge. These early samples are usually discarded and this is referred to as burn-in. The next state of the algorithm depends on its current state and this leads to auto-correlation in the samples. To suppress this auto-correlation, we only retain every r^{th} sample. This is known as thinning. The details of burn-in and thinning are further explained in later sections.

The TAGM MCMC method is computationally intensive and requires at least modest processing power. Leaving the MCMC algorithm to run overnight on a modern desktop is usually sufficient, however this, of course, depends on the particular dataset being analysed. For guidance: it should not be expected that the analysis will finish in just a couple of hours on a medium specification laptop, for example.

To demonstrate the class structure and expected outputs of the TAGM MCMC method, we run a brief analysis on a subset (400 randomly chosen proteins) of the `tan2009r1` dataset from the `pRolocdata`, purely for illustration. This is to provide a bare bones analysis of these data without being held back by computational requirements. We perform a complete demonstration and provide precise details of the analysis of the stem cell dataset considered above in the next section.

```
set.seed(1)
data(tan2009r1)
tan2009r1 <- tan2009r1[sample(nrow(tan2009r1), 400), ]
```

The first step is to run a few MCMC chains (below we use only 2 chains) for a few iterations (we specify 3 iterations in the below code, but typically we would suggest in the order of tens of thousands; see for example the algorithms default settings by typing `?tagmMcmcTrain`) using the `tagmMcmcTrain` function. This function will generate a object of class `MCMCParams`.

```
p <- tagmMcmcTrain(object = tan2009r1, numIter = 3,
                   burnin = 1, thin = 1, numChains = 2)
p
```

```
## Object of class "MCMCParams"
## Method: TAGM.MCMC
## Number of chains: 2
```

Information for each MCMC chain is contained within the chains slot. If needed, this information can be accessed manually. The function `tagmMcmcProcess` processes the `MCMCParams` object and populates the summary slot.

```
p <- tagmMcmcProcess(p)
p
```

```
## Object of class "MCMCParams"
## Method: TAGM.MCMC
## Number of chains: 2
## Summary available
```

The summary slot has now been populated to include basic summaries of the MCMC chains, such as organelle allocations and localisation probabilities. Protein information can be appended to the feature columns of the

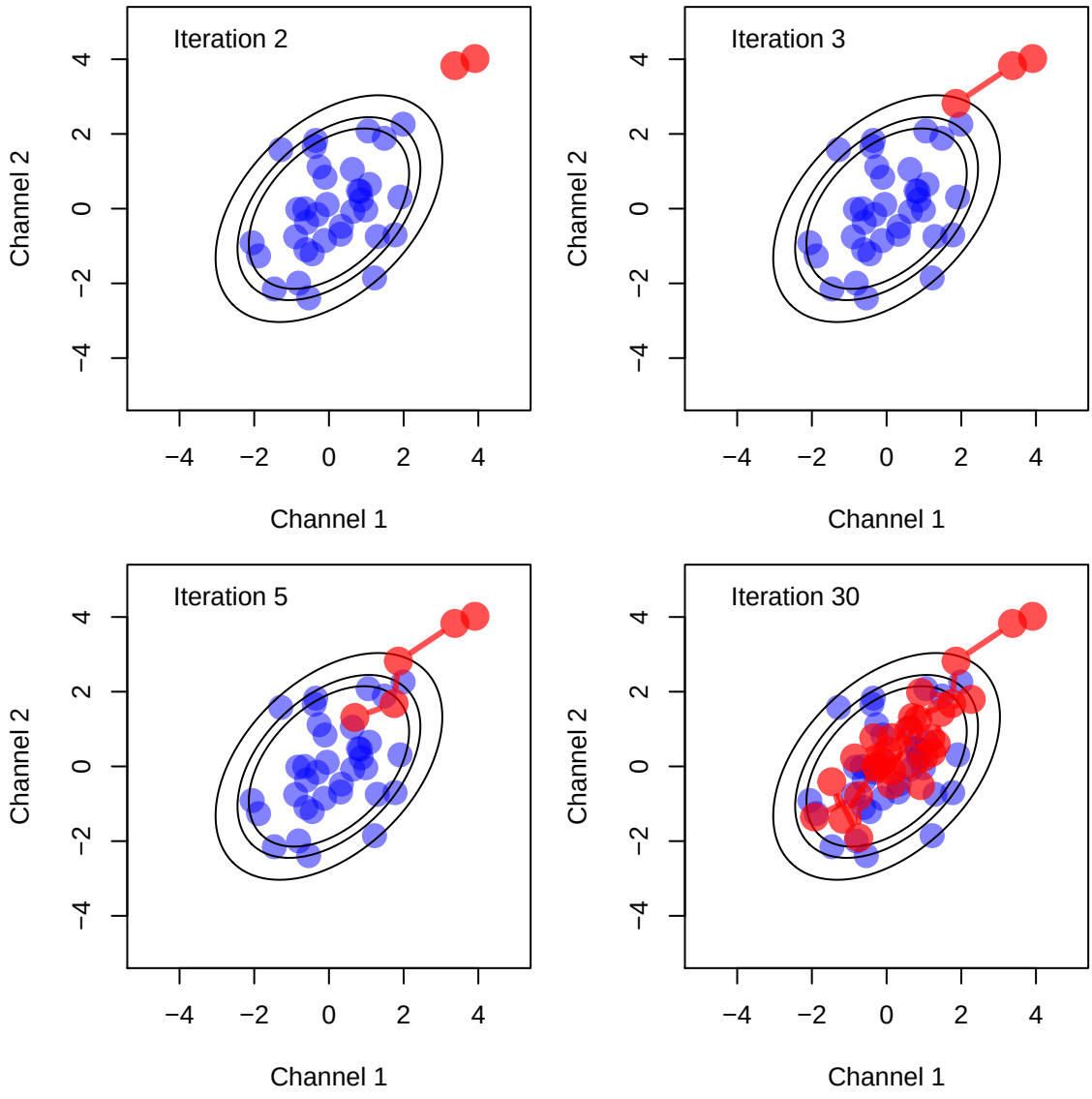

Figure 5: A schematic figure of MCMC sampling. Proteins are coloured in blue and probability ellipses are overlaid representing contours of a probability distribution matching the distribution of the proteins. MCMC samples from this distribution are then coloured in red.

MSnSet by using the tagmPredict function, which extracts the required information from the summary slot of the MCMCParams object.

```
res <- tagmPredict(object = tan2009r1, params = p)
```

We can now access new variables:

- tagm.mcmc.allocation: the TAGM MCMC prediction for the most likely protein sub-cellular annotation.

```
table(fData(res)$tagm.mcmc.allocation)
```

```
##
##  Cytoskeleton            ER         Golgi      Lysosome mitochondrion
##            11            98            20            10            39
##       Nucleus    Peroxisome            PM    Proteasome  Ribosome 40S
##            24             3           106            27            31
##  Ribosome 60S
##            31
```

- tagm.mcmc.probability: the mean posterior probability for the protein sub-cellular allocations.

```
summary(fData(res)$tagm.mcmc.probability)
```

```
##    Min. 1st Qu.  Median    Mean 3rd Qu.    Max.
##  0.3186  0.8667  0.9846  0.9021  1.0000  1.0000
```

We can also access other useful summaries of the MCMC methods:

- tagm.mcmc.outlier the posterior probability for the protein to belong to the outlier component.
- tagm.mcmc.probability.lowerquantile and tagm.mcmc.probability.upperquantile are the lower and upper boundaries to the equi-tailed 95% credible interval of tagm.mcmc.probability.
- tagm.mcmc.mean.shannon a Monte-Carlo averaged Shannon entropy, which is a measure of uncertainty in the allocations.

Methods: *TAGM MCMC* the details

This section explains how to manually manipulate the MCMC output of the TAGM model. In the code chunk below, we load a pre-computed TAGM MCMC model. The data file e14tagm.rda is available online[1] and is not directly loaded into this package due to its size. The file itself if around 500mb, which is too large to directly load into a package.

```
load("e14Tagm.rda")
```

The following code, which is not evaluated dynamically, was used to produce the tagmE14 MCMCParams object. We run the MCMC algorithm for 20,000 iterations with 10,000 iterations discarded for burn-in. We then thin the chain by 20. We ran 6 chains in parallel and so we obtain 500 samples for each of the 6 chains, totalling 3,000 samples. The resulting file is assumed to be in our working directory.

```
e14Tagm <- tagmMcmcTrain(E14TG2aR,
                         numIter = 20000,
                         burnin = 10000,
                         thin = 20,
                         numChains = 6)
```

Manually inspecting the object, we see that it is a MCMCParams object with 6 chains.

[1] https://drive.google.com/open?id=1zozntDhE6YZ-q8wjtQ-lxZ66EEszOGYi

```
e14Tagm
```

```
## Object of class "MCMCParams"
## Method: TAGM.MCMC
## Number of chains: 6
```

Data exploration and convergence diagnostics

Assessing whether or not an MCMC algorithm has converged is challenging. Assessing and diagnosing convergence is an active area of research and throughout the 1990s many approaches were proposed (Geweke 1992; Gelman and Rubin 1992; Roberts and Smith 1994; Brooks and Gelman 1998) and these discussions have been refined in recent years (see (Vats and Knudson 2018), (Vehtari et al. 2019)). We provide a more detailed exploration of this issue, but readers should bear in mind that the methods provided below are diagnostics and cannot guarantee convergence. We direct readers to several important works in the literature discussing the assessment of convergence. Users that do not assess convergence and base their downstream analysis on unconverged chains are likely to obtain poor quality results.

We first assess convergence using a parallel chains approach. We find producing multiple chains is benificial not only for computational advantages but also for analysis of convergence of our chains. As with other authors, we suggest a minimum of 4 chains (Vehtari et al. 2019). This is the default setting in the software. However, in this workflow we run 6 chains to highlight some challenges.

```
## Get number of chains
nChains <- length(e14Tagm)
nChains
```

```
## [1] 6
```

The following code chunks set up a manual convergence diagnostic check. We make use of objects and methods in the package *coda* to perform this analysis (Plummer et al. 2006). Our function below automatically coerces our objects into *coda* for ease of analysis. We first calculate the total number of outliers at each iteration of each chain and, if the algorithm has converged, this number should be the same (or very similar) across all 6 chains.

```
## Convergence diagnostic to see if we need to discard any
## iterations or entire chains: compute the number of outliers for
## each iteration for each chain
out <- mcmc_get_outliers(e14Tagm)
```

We can observe this from the trace plots and histograms for each MCMC chain (figure @ref(fig:mcmctraceHidden)). Unconverged chains should be discarded from downstream analysis.

```
## Using coda S3 objects to produce trace plots and histograms
for (i in seq_len(nChains))
    plot(out[[i]], main = paste("Chain", i), auto.layout = FALSE, col = i)
```

Chains 3, 5 and 6 are centred around an average of 153, with rapid back and forth oscillations. Chain 2 should be immediately discarded, since it has a large jump in the chain with clearly skewed histogram. The other two chains oscillate differently with contrasting quantiles to the 3 chains (3, 5 and 6) that agree with one another, suggesting these chains have yet to converge. We can use the *coda* package to produce summaries of our chains. Here is the `coda` summary for the third chain.

```
## Chains average around 153 outliers
summary(out[[3]])
```

```
##
## Iterations = 1:500
```

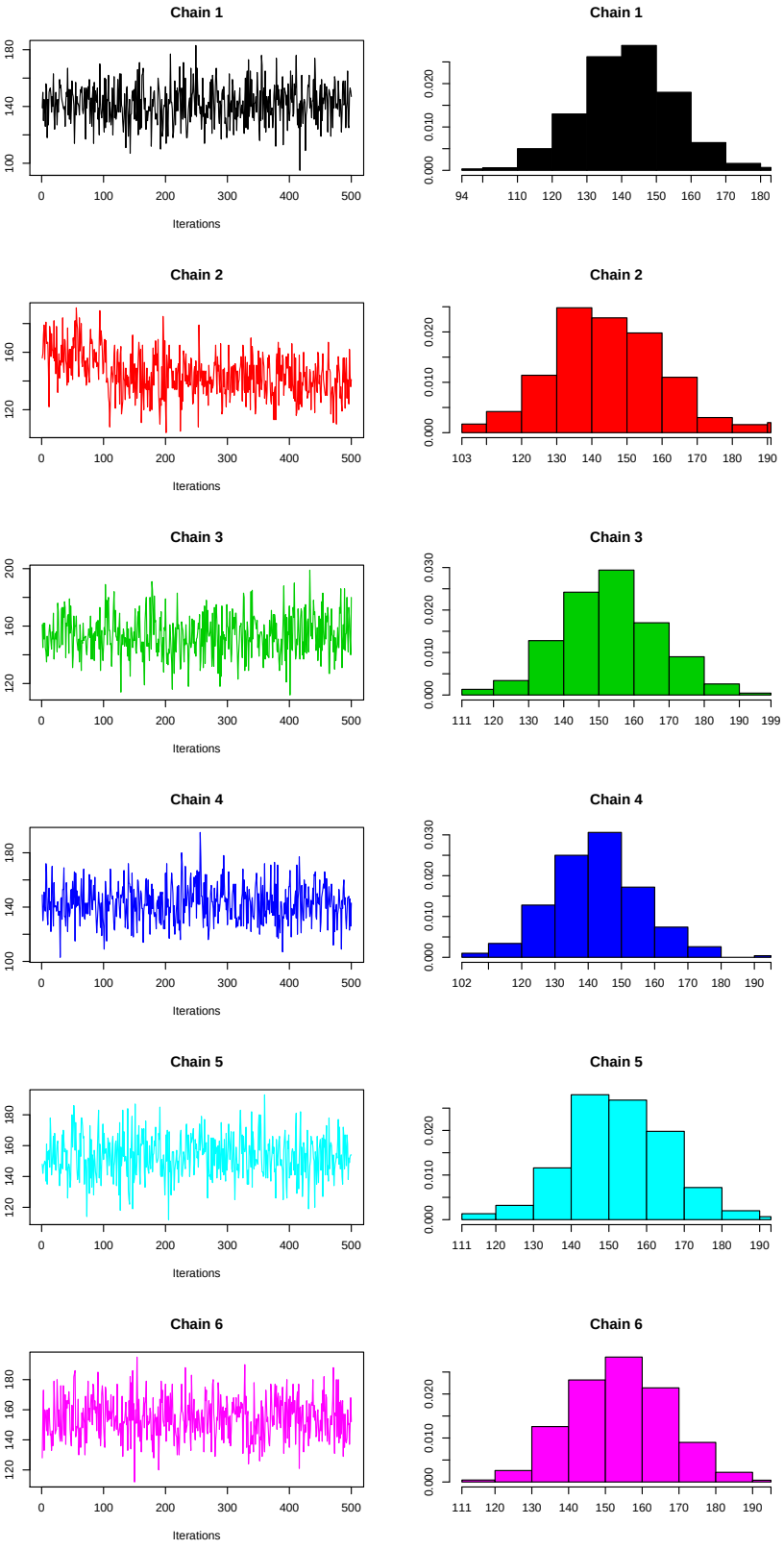

Figure 6: Trace (left) and density (right) of the 6 MCMC chains. 500 iterations were subsampled from the MCMC chains of 20,000 iterations

```
## Thinning interval = 1
## Number of chains = 1
## Sample size per chain = 500
##
## 1. Empirical mean and standard deviation for each variable,
##    plus standard error of the mean:
##
##           Mean             SD       Naive SE Time-series SE
##       153.4520        14.0771         0.6295         0.6820
##
## 2. Quantiles for each variable:
##
##  2.5%   25%   50%   75% 97.5%
##   127   144   153   162   183
```

Applying the Gelman diagnostic

So far, our analysis appears promising. Three of our chains are centred around an average of 153 outliers and there is no observed monotonicity in our output. However, for a more rigorous and unbiased analysis of convergence we can calculate the Gelman diagnostic using the *coda* package (Gelman and Rubin 1992; Brooks and Gelman 1998). This statistic is often referred to as $\hat{R}$ or the potential scale reduction factor. The idea of the Gelman diagnostics is to compare the inter and intra chain variances. The ratio of these quantities should be close to one. A more detailed and in depth discussion can be found in the references. The *coda* package also reports the 95% upper confidence interval of the $\hat{R}$ statistic. In this case, our samples are approximately normally distributed (see histograms on the right in figure @ref(fig:mcmctraceHidden)). The *coda* package allows for transformations to improve normality of the data, and in some cases we set the `transform` argument to apply log transformation. Gelman and Rubin (1992) suggest that chains with $\hat{R}$ value of less than 1.2 are likely to have converged, though recent literature suggests considerably smaller values and a thredhold of 1.01 is likely to lead to more stable and reliable results (Vats and Knudson 2018; Vehtari et al. 2019).

```
gelman.diag(out, transform = FALSE)
```

```
## Potential scale reduction factors:
##
##      Point est. Upper C.I.
## [1,]       1.14       1.32
```

```
gelman.diag(out[c(1, 3, 4, 5, 6)], transform = FALSE)
```

```
## Potential scale reduction factors:
##
##      Point est. Upper C.I.
## [1,]       1.13       1.31
```

```
gelman.diag(out[c(3, 5, 6)], transform = FALSE)
```

```
## Potential scale reduction factors:
##
##      Point est. Upper C.I.
## [1,]          1       1.01
```

In all cases, we see that the Gelman diagnostic for convergence is < 1.2, but only in the final case is it < 1.01. However, the upper confidence interval is 1.32 when all chains are used; 1.31 when chain 2 is removed and when chains 1, 2 and 4 are removed the upper confidence interval is 1.01 indicating that the MCMC algorithm for chains 3, 5 and 6 might have converged.

We can also look at the Gelman diagnostics statistics for groups or pairs of chains. The first line below computes the Gelman diagnostic across the first three chains, whereas the second calculates the diagnostic between chain 3 and chain 5.

```
gelman.diag(out[1:3], transform = FALSE) # the upper C.I is 1.62
```

```
## Potential scale reduction factors:
##
##      Point est. Upper C.I.
## [1,]       1.22       1.62
```

```
gelman.diag(out[c(3, 5)], transform = TRUE) # the upper C.I is 1.01
```

```
## Potential scale reduction factors:
##
##      Point est. Upper C.I.
## [1,]       1.01       1.01
```

To assess another summary statistic, we can look at the mean component allocation at each iteration of the MCMC algorithm and as before we produce trace plots of this quantity (figure @ref(fig:mcmctrace2hidden)).

```
meanAlloc <- mcmc_get_meanComponent(e14Tagm)
```

```
for (i in seq_len(nChains))
    plot(meanAlloc[[i]], main = paste("Chain", i), auto.layout = FALSE, col = i)
```

As before we can produce summaries of the data.

```
summary(meanAlloc[[1]])
```

```
##
## Iterations = 1:500
## Thinning interval = 1
## Number of chains = 1
## Sample size per chain = 500
##
## 1. Empirical mean and standard deviation for each variable,
##    plus standard error of the mean:
##
##           Mean             SD       Naive SE Time-series SE
##       5.686713       0.059112       0.002644       0.002644
##
## 2. Quantiles for each variable:
##
##  2.5%   25%   50%   75% 97.5%
## 5.552 5.646 5.692 5.728 5.795
```

We can already observed that there are some slight differences between these chains, which raises suspicion that some of the chains may not have converged. For example each chain appears to be centred around 5.7, but chains 2 and 4 have clear jumps in the their trace plots. To be more precise, we note the jump that occurs are between iteration 100-150 in chain 2 and between iteration 200-250 in chain 4. For a more quantitative analysis, we again apply the Gelman diagnostics to these summaries.

```
gelman.diag(meanAlloc)
```

```
## Potential scale reduction factors:
##
##      Point est. Upper C.I.
## [1,]          1       1.01
```

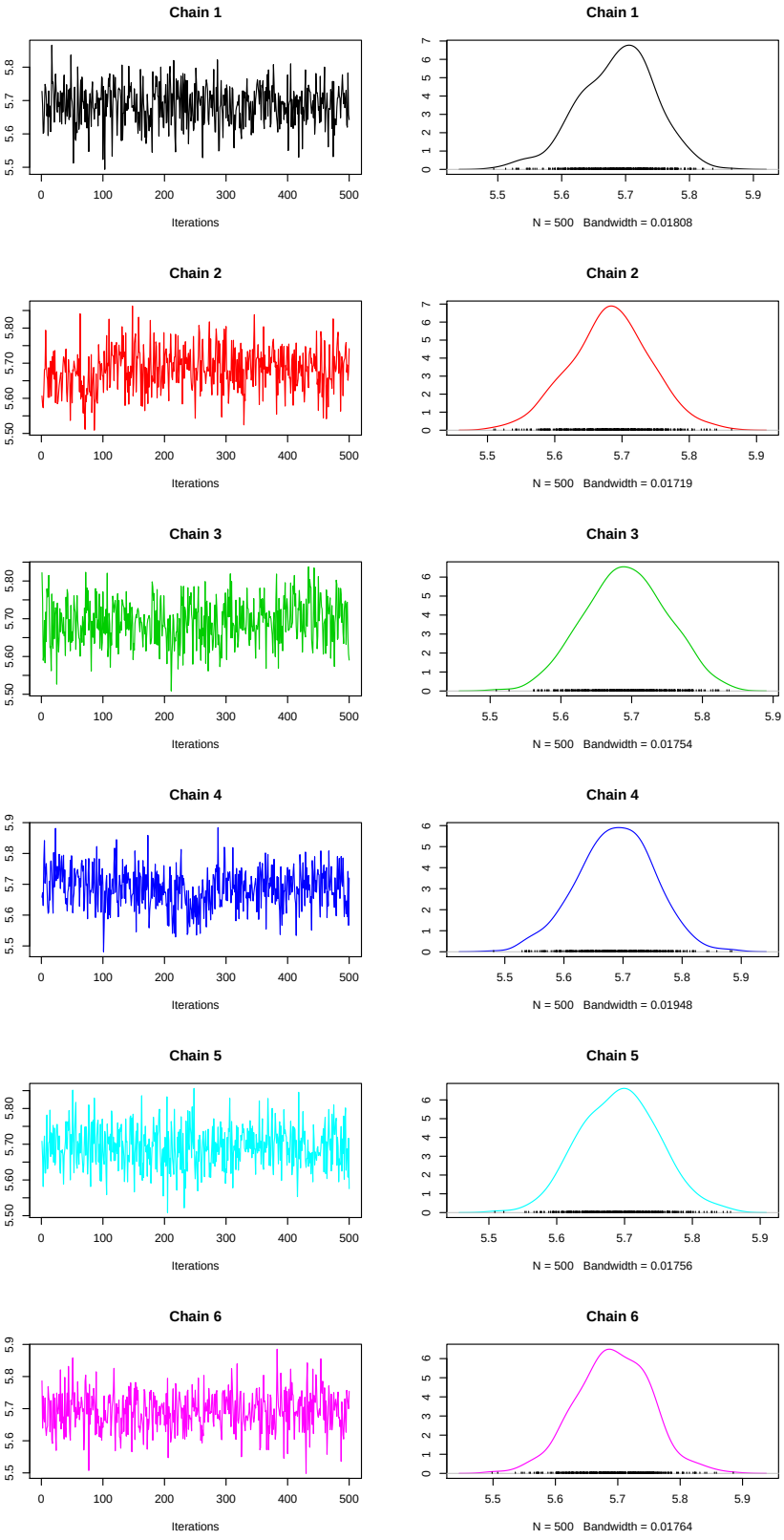

Figure 7: Trace (left) and density (right) of the mean component allocation of the 6 MCMC chains. 500 iterations were subsampled from the MCMC chains of 20,000 iterations.

The above values are close to 1 and so there are no significant differences between the chains. As observed previously, chains 2 and 4 look quite different from the other chains and so we recalculate the diagnostic excluding these chains. The computed Gelman diagnostic below suggest that chains 3, 5 and 6 have converged and that we should discard chains 1, 2 and 4 from further analysis.

```
gelman.diag(meanAlloc[c(3, 5, 6)])
```

```
## Potential scale reduction factors:
##
##      Point est. Upper C.I.
## [1,]          1          1
```

For a further check, we can look at the mean outlier probability at each iteration of the MCMC algorithm and again computing the Gelman diagnostics between chains 3, 5 and 6. An $\hat{R}$ statistic of 1 is indicative of convergence, since it is less than the recommended value of 1.01.

```
meanoutProb <- mcmc_get_meanoutliersProb(e14Tagm)
gelman.diag(meanoutProb[c(3, 5, 6)])
```

```
## Potential scale reduction factors:
##
##      Point est. Upper C.I.
## [1,]          1       1.01
```

Applying the Geweke diagnostic

Along with the Gelman diagnostic, which uses parallel chains, we can also apply a single chain analysis using the Geweke diagnostic (Geweke 1992). The Geweke diagnostic tests to see whether the mean calculated from the first 10% of iterations is significantly different from the mean calculated from the last 50% of iterations. If they are significantly different, at say a level 0.01, then this is evidence that particular chains have not converged. The following code chunk calculates the Geweke diagnostic for each chain on the summarising quantities we have previously computed.

```
geweke_test(out)
```

```
##           chain 1      chain 2  chain 3    chain 4    chain 5    chain 6
## z.value 0.5749775 8.816632e+00 0.470203 -0.3204500 -0.6270787 -0.7328168
## p.value 0.5653065 1.179541e-18 0.638210  0.7486272  0.5306076  0.4636702
```

```
geweke_test(meanAlloc)
```

```
##           chain 1       chain 2    chain 3    chain 4   chain 5    chain 6
## z.value 1.1952967 -3.3737051063 -1.2232102 2.48951993 0.3605882 -0.1358850
## p.value 0.2319711  0.0007416377  0.2212503 0.01279157 0.7184073  0.8919122
```

```
geweke_test(meanoutProb)
```

```
##           chain 1      chain 2   chain 3    chain 4    chain 5     chain 6
## z.value 0.1785882 1.205500e+01 0.6189637 -0.5164987 -0.2141086 -0.02379004
## p.value 0.8582611 1.825379e-33 0.5359403  0.6055062  0.8304624  0.98102008
```

The first test suggests chain 2 has not converged, since the p-value is less than 10^{-10} suggesting that the mean in the first 10% of iterations is significantly different from those in the final 50%. Moreover, the second test and third tests also suggest that chain 2 has not converged. Furthermore, for the second test chain 4 has a marginally small p-value, providing further evidence that this chain is of low quality. These convergence diagnostics are not limited to the quantities we have computed here and further diagnostics can be performed on any summary of the data.

An important question to consider is whether removing an early portion of the chain might lead to an improvement of the convergence diagnostics. This might be particularly relevant if a chain converges some iterations after our orginally specified `burn-in`. For example, let us take the second Geweke test above, which suggested chains 2 and 4 had not converged and see if discarding the initial 10% of the chain improves the statistic. The function below removes 50 samples, known as `burn-in`, from the beginning of each chain and the output shows that we now have 450 samples in each chain. In practice, as 2 chains are sufficient for good posterior estimates and convergence we could simply discard chains 2 and 4 and proceed with downstream analysis with the remaining chains.

```
burn_e14Tagm <- mcmc_burn_chains(e14Tagm, 50)
chains(burn_e14Tagm)
```

```
## Object of class "MCMCChains"
##  Number of chains: 6
```

```
chains(burn_e14Tagm)[[4]]
```

```
## Object of class "MCMCChain"
##  Number of components: 10
##  Number of proteins: 1663
##  Number of iterations: 450
```

The following function recomputes the number of outliers in each chain at each iteration of each Markov-chain.

```
out2 <- mcmc_get_outliers(burn_e14Tagm)
```

The code chunk below computes the Geweke diagnostic for this new truncated chain and demonstrates that chain 4 has an improved Geweke diagnostic, whilst chain 2 does not. Thus, in practice, it maybe useful to remove iterations from the beginning of the chain. However, as chain 4 did not pass the Gelman diagnostics we still discard it from downstream analysis.

```
geweke_test(out2)
```

```
##            chain 1      chain 2    chain 3   chain 4   chain 5   chain 6
## z.value -0.1455345 6.379618e+00 -1.6392215 0.3836940 0.1241201 0.6654703
## p.value  0.8842889 1.775298e-10  0.1011671 0.7012053 0.9012202 0.5057497
```

In this section, we have highlighted that assessing convergence is an essential part of Bayesian analysis. As well as the summaries considered here, we recommend that users assess other posterior summaries of the data. Since the best practices for assessing convergence also change overtime, we also suggest searching the literature for current consensus.

Processing converged chains

Having made an assessment of convergence, we decide to discard chains $1, 2$ and 4 from any further analysis. The code chunk below removes these chains and creates a new object to store the converged chains.

```
removeChain <- c(1, 2, 4) # The chains to be removed
e14Tagm_converged <- e14Tagm[-removeChain] # Create new object
```

The `MCMCParams` object can be large and therefore if we have a large number of samples we may want to subsample our chain, known as *thinning*, to reduce the number of samples. Thinning also has another purpose. We may desire independent samples from our posterior distribution but the MCMC algorithm produces auto-correlated samples. Thinning can be applied to reduce the auto-correlation between samples. The code chunk below, which is not evaluated, demonstrates retaining every 5^{th} iteration. Recall that we thinned by 20 when we first ran the MCMC algorithm.

```
e14Tagm_converged_thinned <- mcmc_thin_chains(e14Tagm_converged, freq  = 5)
```

We initially ran 6 chains and, after having made an assessment of convergence, we decided to discard 3 of the chains. We desire to make inference using samples from all 3 chains, since this leads to better posterior estimates. In their current class structure all the chains are stored separately, so the following function pools all sample for all chains together to make a single longer chain with all samplers. Pooling a mixture of converged and unconverged chains is likely to lead to poor quality results so should be done with care.

```
e14Tagm_converged_pooled <- mcmc_pool_chains(e14Tagm_converged)
e14Tagm_converged_pooled
```

```
## Object of class "MCMCParams"
## Method: TAGM.MCMC
## Number of chains: 1
```

```
e14Tagm_converged_pooled[[1]]
```

```
## Object of class "MCMCChain"
##  Number of components: 10
##  Number of proteins: 1663
##  Number of iterations: 1500
```

To populate the summary slot of the converged and pooled chain, we can use the `tagmMcmcProcess` function. As we can see from the object below a summary is now available. The information now available in the summary slot was detailed in the previous section. We note that if there is more than 1 chain in the `MCMCParams` object then the chains are automatically pooled to compute the summaries.

```
e14Tagm_converged_pooled <- tagmMcmcProcess(e14Tagm_converged_pooled)
e14Tagm_converged_pooled
```

```
## Object of class "MCMCParams"
## Method: TAGM.MCMC
## Number of chains: 1
## Summary available
```

To create new feature columns in the `MSnSet` and append the summary information, we apply the `tagmPredict` function. The `probJoint` argument indicates whether or not to add probabilistic information for all organelles for all proteins, rather than just the information for the most probable organelle. The outlier probabilities are also returned by default, but users can change this using the `probOutlier` argument.

```
E14TG2aR <- tagmPredict(object = E14TG2aR,
                        params = e14Tagm_converged_pooled,
                        probJoint = TRUE)
head(fData(E14TG2aR))
```

```
##        Uniprot.ID UniprotName
## Q62261     Q62261 SPTB2_MOUSE
## Q9JHU4     Q9JHU4 DYHC1_MOUSE
## Q9QXS1     Q9QXS1  PLEC_MOUSE
## P16546     P16546 SPTA2_MOUSE
## Q69ZN7     Q69ZN7  MYOF_MOUSE
## P30999     P30999 CTND1_MOUSE
##                                      Protein.Description Peptides PSMs
## Q62261 Spectrin beta chain, brain 1 (multiple isoforms)       42   42
## Q9JHU4               Cytoplasmic dynein 1 heavy chain 1       33   33
## Q9QXS1                       Isoform PLEC-1I of Plectin       33   33
## P16546  Spectrin alpha chain, brain (multiple isoforms)       32   32
## Q69ZN7                   Myoferlin (multiple isoforms)       28   28
```

```
## P30999              Catenin delta-1 (multiple isoforms)       24   24
##        GOannotation markers.orig         markers   tagm.map.allocation
## Q62261      PLM-SKE      unknown         unknown Endoplasmic reticulum
## Q9JHU4          SKE      unknown         unknown   Nucleus - Chromatin
## Q9QXS1      unknown      unknown         unknown       Plasma membrane
## P16546  PLM-SKE-CYT      unknown         unknown   Nucleus - Chromatin
## Q69ZN7          VES      unknown         unknown       Plasma membrane
## P30999      PLM-NUC          PLM Plasma membrane       Plasma membrane
##        tagm.map.probability tagm.map.outlier  tagm.mcmc.allocation
## Q62261         8.165817e-09     0.9999999857 Endoplasmic reticulum
## Q9JHU4         9.996798e-01     0.0003202255   Nucleus - Chromatin
## Q9QXS1         1.250898e-06     0.9999987491            Proteasome
## P16546         4.226696e-07     0.9999995462 Endoplasmic reticulum
## Q69ZN7         9.994502e-01     0.0001083130       Plasma membrane
## P30999         1.000000e+00     0.0000000000       Plasma membrane
##        tagm.mcmc.probability tagm.mcmc.probability.lowerquantile
## Q62261             0.5765793                          0.0020296117
## Q9JHU4             0.9738206                          0.7594516090
## Q9QXS1             0.4957129                          0.0002886457
## P16546             0.5214374                          0.0014041362
## Q69ZN7             0.9997025                          0.9981794326
## P30999             1.0000000                          1.0000000000
##        tagm.mcmc.probability.upperquantile tagm.mcmc.mean.shannon
## Q62261                           0.9992504            0.201623229
## Q9JHU4                           0.9998822            0.081450206
## Q9QXS1                           0.9947100            0.447665536
## P16546                           0.9946959            0.252833750
## Q69ZN7                           0.9999954            0.002395147
## P30999                           1.0000000            0.000000000
##        tagm.mcmc.outlier tagm.mcmc.joint.40S Ribosome
## Q62261      2.547793e-01                4.401228e-10
## Q9JHU4      3.335134e-05                1.936225e-18
## Q9QXS1      6.423799e-01                2.213861e-07
## P16546      2.119112e-01                1.576023e-09
## Q69ZN7      7.274103e-06                3.510523e-22
## P30999      0.000000e+00                0.000000e+00
##        tagm.mcmc.joint.60S Ribosome tagm.mcmc.joint.Cytosol
## Q62261                2.778620e-07            2.650861e-12
## Q9JHU4                1.645727e-21            1.887645e-17
## Q9QXS1                1.495170e-01            9.062280e-09
## P16546                3.150122e-06            1.471329e-08
## Q69ZN7                5.152312e-16            2.063009e-24
## P30999                0.000000e+00            0.000000e+00
##        tagm.mcmc.joint.Endoplasmic reticulum tagm.mcmc.joint.Lysosome
## Q62261                          5.765793e-01             1.108757e-11
## Q9JHU4                          1.548053e-17             5.577415e-24
## Q9QXS1                          1.768681e-04             1.150706e-04
## P16546                          5.214374e-01             3.687975e-09
## Q69ZN7                          8.397027e-09             2.974966e-04
## P30999                          0.000000e+00             0.000000e+00
##        tagm.mcmc.joint.Mitochondrion tagm.mcmc.joint.Nucleus - Chromatin
## Q62261                 5.020528e-08                          4.231731e-01
## Q9JHU4                 2.835919e-22                          9.738206e-01
## Q9QXS1                 5.832273e-19                          7.920397e-03
```

```
## P16546                  4.522032e-08                          4.776913e-01
## Q69ZN7                  6.143974e-39                          4.872032e-21
## P30999                  0.000000e+00                          0.000000e+00
##        tagm.mcmc.joint.Nucleus - Nucleolus tagm.mcmc.joint.Plasma membrane
## Q62261                        1.279255e-05                       1.914808e-11
## Q9JHU4                        2.617943e-02                       3.514851e-29
## Q9QXS1                        1.130580e-05                       3.465462e-01
## P16546                        3.448558e-05                       2.489652e-07
## Q69ZN7                        7.042891e-30                       9.997025e-01
## P30999                        0.000000e+00                       1.000000e+00
##        tagm.mcmc.joint.Proteasome
## Q62261               2.345204e-04
## Q9JHU4               7.841425e-11
## Q9QXS1               4.957129e-01
## P16546               8.333595e-04
## Q69ZN7               1.003778e-10
## P30999               0.000000e+00
```

Priors

Introduction

Bayesian analysis requires users to specify prior information about the parameters. This may appear to be a challenging task; however, good default options are often possible. Should expert information or domain specific knowledge be available for any of these priors then the users should provide this, otherwise we have found that the default choices work well in practice. The priors also provide regularisation and shrinkage to avoid overfitting. Given enough data the likelihood overwhelms the prior and the influence of the prior is weak.

Empirical Bayes priors on the mixture components

We place a normal inverse-Wishart prior on the parameters of the mutivariate normal mixture components. The normal inverse-Wishart prior has 4 hyperparameters that must be specified. These are: the prior mean `mu0` expressing the prior location of each organelle; a prior shrinkage `lambda0`, which is a scalar expressing uncertainty in the prior mean; the prior degrees of freedom `nu0`; and a scale prior `S0` on the covariance. Together, `nu0` and `S0` specify the prior variability on organelle covariances. The same prior distribution is assumed for the parameters of all mutivariate normal mixture components.

An empirical Bayes approach is used to set these priors, which is pragmatic approach when little prior information is known. The choices for these priors are based on the recommendation by (Fraley and Raftery 2005). The prior mean `mu0` is set to be the mean of the data. `lambda0` is set to be 0.01 meaning some uncertainty in the covariance is propagated to the mean, increasing `lambda0` increases shrinkage towards the prior. `nu0` is set to the number of feature variables plus 2, which is the smallest integer value that ensures a finite covariance matrix. The prior scale matrix $S0$ is set to

$$S_0 = \frac{\text{diag}(\frac{1}{n}\sum(X - \bar{X})^2)}{K^{1/D}}, \tag{1}$$

and represents a diffuse prior on the covariance. Another good choice, which is often used, is a constant multiple of the identity matrix.

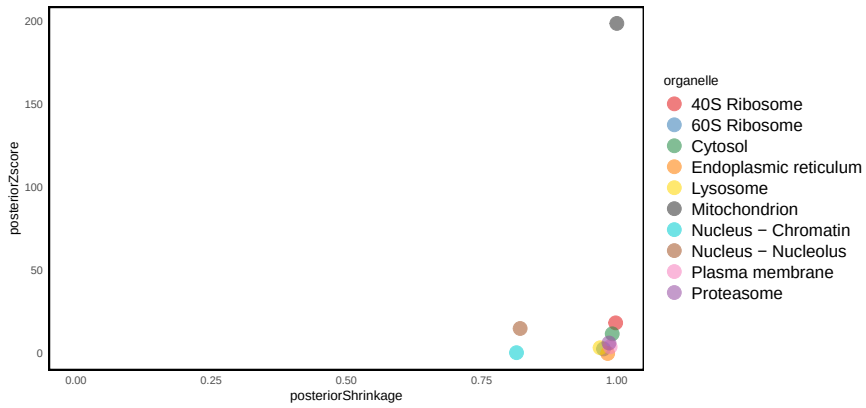

Figure 8: Scatter plot of the posterior Shrinkage against the posterior z-score for the mixing proportions of the model

Prior on the mixing proportions

The prior on the mixing proprotions is the Dirichlet distribution with concentration parameters `beta0` set to 1 for each organelle. Another reasonable choice would be the non-informative Jeffery's prior for the Dirichlet hyperparameter, which sets `beta0` to 0.5 for each organelle. The following discussion assesses the quality and sensitivity of our prior choice. We compute the posterior z-score which assesses how the posterior recovers the assumed true model configuration with small values for the posterior z-score suggesting good calibration (Betancourt 2018). We also compute the posterior shrinkage, which quantifies how much is learnt about a given parameter from the data (Betancourt 2018). Values of the posterior shrinkage close to 1 suggest that the parameter values are strongly informed by the data.

```
mixing_posterior_check(object = E14TG2aR, params = e14Tagm_converged_pooled[[1]], priors = e14Tagm@prio
```

We see that most parameter values concentrate in the lower right hand corner of the plot, which suggests good shrinkage and calibration. However, the parameter for the mitochondrion is located in the top right of the plot suggesting the posterior deviates from the prior. The biological interpretation for this is that the experiment resolved the mitochondrial proteins extremely well and thus allocated many more proteins to this class than perhaps we might have expected. This could be remedied with a more informative prior. If we prefer to use an informative prior, rather than a non-informative prior, it is practical to use information from previous data. To demonstrate this, we consider another experiment on mouse pluripotent stem cells and examine the number of proteins that were allocated to each subcellular niche. The code chunk below extracts this information from another spatial proteomics experiment.

```
data("hyperLOPIT2015")
priordata <- table(fData(hyperLOPIT2015)$final.assignment)
priordata
```

```
##
##                          40S Ribosome
##                                    48
##                          60S Ribosome
##                                    62
##                     Actin cytoskeleton
##                                    46
##                                Cytosol
##                                   339
## Endoplasmic reticulum/Golgi apparatus
```

```
##                                 426
##                            Endosome
##                                  60
##                 Extracellular matrix
##                                  17
##                             Lysosome
##                                  80
##                       Mitochondrion
##                                 585
##                  Nucleus - Chromatin
##                                 297
##               Nucleus - Non-chromatin
##                                 396
##                           Peroxisome
##                                  25
##                      Plasma membrane
##                                 392
##                           Proteasome
##                                  34
##                              unknown
##                                2225
```

It is clear that the allocations are not uniformly distributed across the classes and that the mitochondrion has more allocations than the other subcellular niches. However, we also do not have prior information on all the classes. The Dirichlet distribution can be interpreted as specifiying the prior relative proportions of the number of proteins allocated to each niche. For the classes where we have no information, we assume equal uniform allocations. First, we compute the number of proteins in this experiment. Then create a vector with proteins allocated equally to each class.

```
N <- nrow(unknownMSnSet(E14TG2aR)) # number of proteins
K <- length(getMarkerClasses(E14TG2aR)) # number of subcellular niches
beta_uninformed <- rep(N/K, K) # uninformative beta0, proteins allocated symmetrically
names(beta_uninformed) <- getMarkerClasses(E14TG2aR)
```

The code chunk below extracts the data for which we have prior information.

```
shared_info <- intersect(getMarkerClasses(hyperLOPIT2015), getMarkerClasses(E14TG2aR))
informativePrior <- priordata[shared_info] # extracts useful information from other dataset
```

We then reweight the prior number of proteins allocated to each class by their relative proportions in the other dataset. We then use this information to create an informative prior.

```
beta_informed <- beta_uninformed
beta_informed[shared_info] <- sum(beta_uninformed[shared_info]) * informativePrior/sum(informativePrior
```

Now, we can check that this prior has captured our beliefs correctly, mainly that the mitchondrion should have more allocations than the other subcellular niches and that distribution is not symmetric. To do this, we simulate 10000 values from the informative prior and compute the expected (prior) number of proteins allocated to each niche.

```
prior_simulation <- colMeans(gtools::rdirichlet(n = 10000, alpha = beta_informed) * N)
names(prior_simulation) <- getMarkerClasses(E14TG2aR)
prior_simulation
```

```
##          40S Ribosome          60S Ribosome               Cytosol
##               34.72586               44.99799              245.62171
## Endoplasmic reticulum              Lysosome         Mitochondrion
```

```
##             166.50286              57.99014             423.32247
##   Nucleus - Chromatin   Nucleus - Nucleolus       Plasma membrane
##             215.53612             166.26266             283.48035
##            Proteasome
##              24.55985
```

It is clear that this prior captures the information that the mitochondrion has more allocations than the other subcellular niches and that the allocations across the classes are not symmetric. It is useful to note that many spatial proteomics datasets can be found in the `pRolocdata` package from which useful information could be extracted.

Prior on the proportion of outlier proteins

The prior for the proportion of outlier proteins is a $\mathcal{B}(u, v)$ distribution. The default for $u = 2$ and the default for $v = 10$. This represents the reasonable belief that $\frac{u}{u+v} = \frac{1}{6}$ proteins *a priori* might be an outlier and we believe is unlikely that more than 50% of proteins are outliers, which was elicited from expert domain knowledge and analysis of previous datasets. Decreasing the value of v, represents more uncertainty about the number of proteins that are outliers.

To visualise that this prior captures these beliefs, we simulate from the prior and produce a histogram.

```
x <- rbeta(n = 1500, shape1 = 2, shape2 = 10)
gg <- ggplot(data.frame(x), aes(x)) + geom_histogram(fill = "darkgreen", col = "black") +
      theme_minimal() +
      theme(panel.grid.major = element_blank(), panel.grid.minor = element_blank(),
            panel.border = element_rect(colour = "black", fill = NA, size = 1),
            plot.title = element_text(hjust = 0.5, size = 20),
            legend.text=element_text(size = 14)) +
      ggtitle(label = "Histogram of simulations from the prior") + xlim(c(-0.05, 1))
gg
```

```
## `stat_bin()` using `bins = 30`. Pick better value with `binwidth`.
```

```
## Warning: Removed 2 rows containing missing values (geom_bar).
```

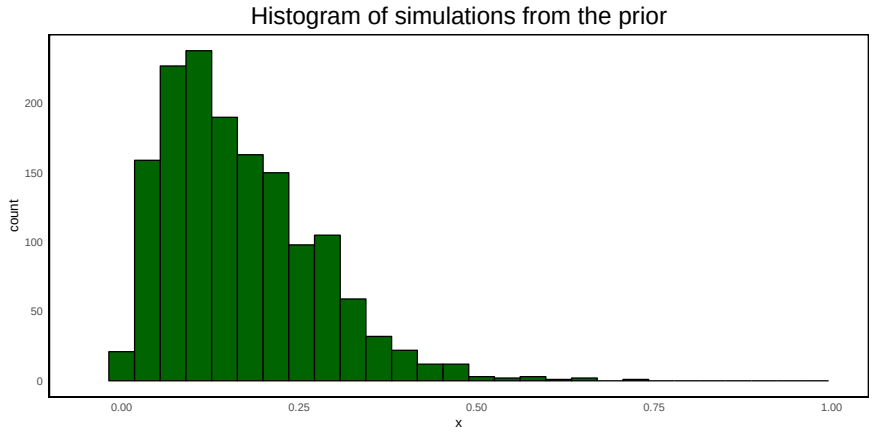

The probability that more than 50% of the proteins are outliers is small but non-zero. The probability there are fewer than 1% outliers is also small. These quantiles can be used to calibrate the prior beliefs.

```
pbeta(0.5, shape1 = 2, shape2 = 10, lower.tail = FALSE) # more than 50% outliers
```

```
## [1] 0.005859375
```

```
pbeta(0.01, shape1 = 2, shape2 = 10, lower.tail = TRUE) # fewer than 1% outliers
```

```
## [1] 0.005179717
```

Now we turn to the posterior distribution for this quantity of interest and overlay onto the prior.

```
out <- mcmc_get_outliers(e14Tagm_converged_pooled)
propout <- out[[1]]/nrow(unknownMSnSet(E14TG2aR))
df <- data.frame(x = c(x, propout), y = as.factor(rep(c("prior", "posterior"), each = 1500)))
gg <- ggplot(df, aes(x = x, fill = y)) + geom_histogram(alpha = 0.7, col = "black", position = "identity
      theme_minimal() +
      theme(panel.grid.major = element_blank(), panel.grid.minor = element_blank(),
           panel.border = element_rect(colour = "black", fill = NA, size = 1),
           plot.title = element_text(hjust = 0.5, size = 20),
           legend.text=element_text(size = 14)) + labs(fill = "Distribution") +
      scale_fill_manual(values = c("purple", "darkgreen")) +
      ggtitle(label = "Histogram of samples from the prior and posterior") + xlim(c(-0.05, 1))
gg
```

```
## Warning: Removed 4 rows containing missing values (geom_bar).
```

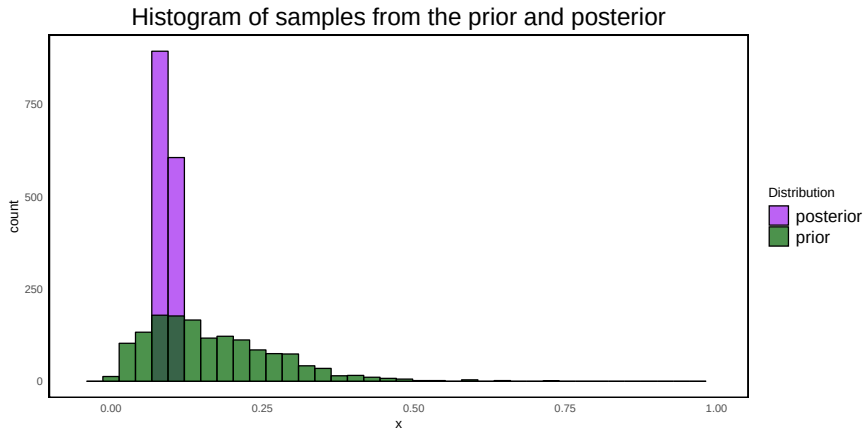

It is clear that the prior and posterior concentrate in the same region, and are thus not in conflict. The variance of the posterior is clearly smaller than that of the prior and so there is high posterior shrinkage. One could argue that the prior is too diffuse to provide regularisation; however, specifying a tighter prior risks biasing the model away from the data generating mechanism.

Analysis, visualisation and interpretation of results

Now that we have a single pooled chain of samples from a converged MCMC algorithm, we can begin to analyse the results. Preliminary analysis includes visualising the allocated organelle and localisation probability of each protein to its most probable organelle, as shown on figure @ref(fig:mcmcpca).

```
par(mfrow = c(1, 2))
plot2D(E14TG2aR, fcol = "tagm.mcmc.allocation",
       cex = fData(E14TG2aR)$tagm.mcmc.probability,
       main = "TAGM MCMC allocations")
addLegend(E14TG2aR, fcol = "markers",
          where = "topleft", ncol = 2, cex = 0.6)

plot2D(E14TG2aR, fcol = "tagm.mcmc.allocation",
```

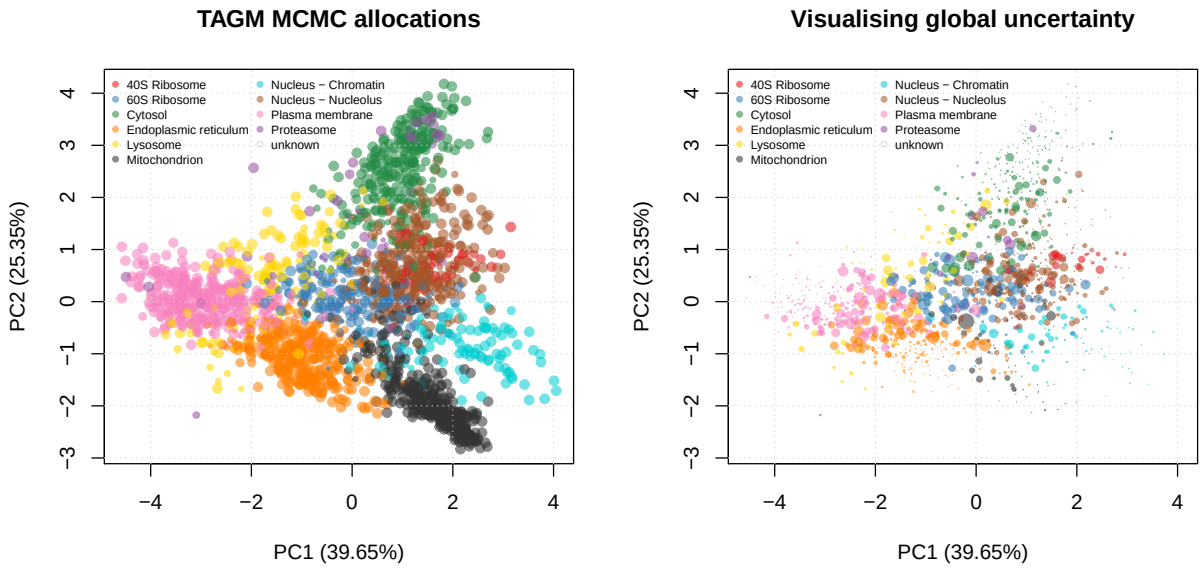

Figure 9: TAGM MCMC allocations. On the left, point size have been scaled based on allocation probabilities. On the right, the point size have been scaled based on the global uncertainty using the mean Shannon entropy.

```
       cex = fData(E14TG2aR)$tagm.mcmc.mean.shannon,
       main = "Visualising global uncertainty")
addLegend(E14TG2aR, fcol = "markers",
          where = "topleft", ncol = 2, cex = 0.6)
```

We can visualise other summaries of the data including a Monte-Carlo averaged Shannon entropy, as shown in figure @ref(fig:mcmcpca) on the right. This is a measure of uncertainty and proteins with greater Shannon entropy have more uncertainty in their localisation. The Shannon Entropy (and hence uncertainty) is greatest when all localisation are equiprobable and lowest when the probabilities are concentrated on a single localisation. For additional discussion, we refer readers to Crook et al. (2018) and Oliver M Crook et al. (2019) and references therein. We observe global patterns of uncertainty, particularly in areas where organelle boundaries overlap. There are also regions of low uncertainty indicating little doubt about the localisation of these proteins.

We are also interested in the relationship between localisation probability to the most probable class and the Shannon entropy. Even though the two quantities are evidently correlated there is still considerable spread. Thus it is important to base inference not only on localisation probability but also a measure of uncertainty, for example the Shannon entropy. Proteins with low Shannon entropy have low uncertainty in their localisation, whilst those with higher Shannon entropy have uncertain localisation. Since multi-localised proteins have uncertain localisation to a single subcellular niche, exploring the Shannon can aid in identifying multi-localised proteins. Examples of well characterised multi-localising proteins from the literature are discussed in (Crook et al. 2018). The interpretation of uncertain allocations in relation to multi-localisation is further discussed in (Crook et al. 2018; Oliver M Crook et al. 2019).

```
cls <- getStockcol()[as.factor(fData(E14TG2aR)$tagm.mcmc.allocation)]
plot(fData(E14TG2aR)$tagm.mcmc.probability,
     fData(E14TG2aR)$tagm.mcmc.mean.shannon,
     col = cls, pch = 19,
     xlab = "Localisation probability",
     ylab = "Shannon entropy")
```

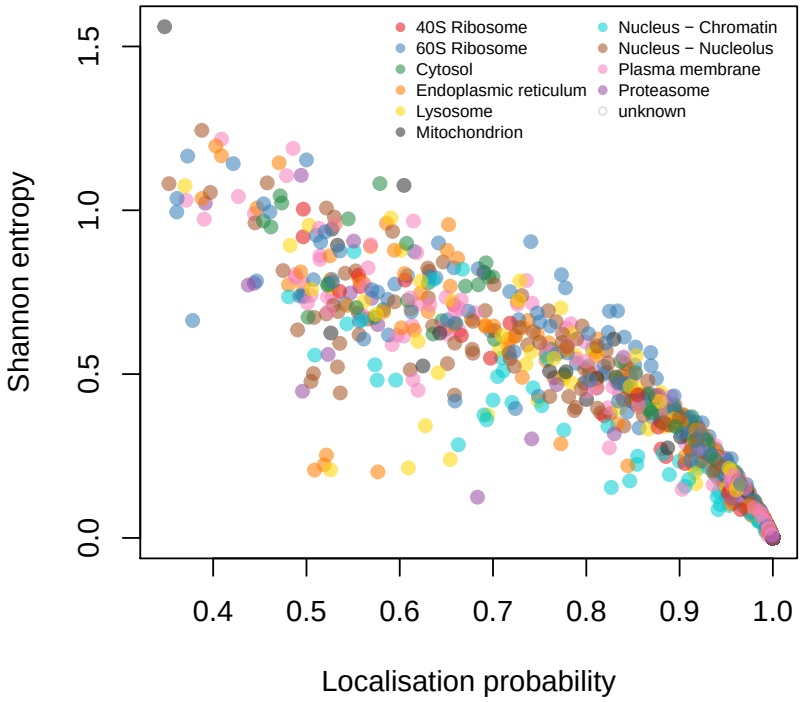

Figure 10: Shannon entropy and localisation probability.

```
addLegend(E14TG2aR, fcol = "markers",
          where = "topright", ncol = 2, cex = 0.6)
```

There are further ways in which we can visualise the uncertainty quantified by the Bayesian analysis. For example, we can use the samples from the MCMC algorithm to visualise the uncertainty in the mean localisation of each organelle/niche on a PCA plot. At each iteration of the MCMC, we compute the mean for each organelle as the mean of all associated proteins to that organelle. These data are then projected on to the PCA plot, having aligned them across the random samples (see (Borg and Groenen 2003), as well as (Ren et al. 2017) and (Nguyen and Holmes 2019) for similar examples).

```
nicheMeans2D(object = E14TG2aR, params = e14Tagm_converged_pooled[[1]], prior = e14Tagm_converged_poole
```

The main quantity of interest is posterior localisation probability of each protein to each organelle. However, visualising how these probabilities vary in different regions of data space are be challenging, especially with large numbers of proteins. Furthermore, interrogating individual proteins one by one can be cumbersome. Thus, we consider visualising how the probabilities vary across different regions of the PCA plot. To perform this analysis, we first compute the underlying coordinates of the whole data in PC space. We proceed by linearly interpolating a regular grid in this coordinate system. To obtain the localisation probabilties on this grid, we use a Nadaraya-Watson kernel smoother (Nadaraya 1964; Watson 1964) with Wendland covariance (Wendland 1995), where a fast Fourier transform is used to accelerate computations (Stein 1999; Gneiting 2002). A contour plot, in the PC coordinates, of these probabilities is then visualised, where the distribution for each organelle is coloured accordingly. The code chunk below produces this plot.

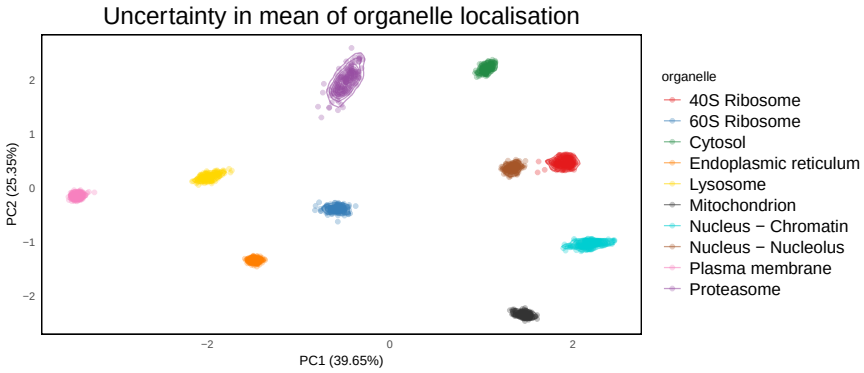

Figure 11: Visualising uncertainty in the mean of each subcellular niche. The pointers correspond to results from different iterations of the MCMC algorithm and are coloured according to the corresponding subcellular niche

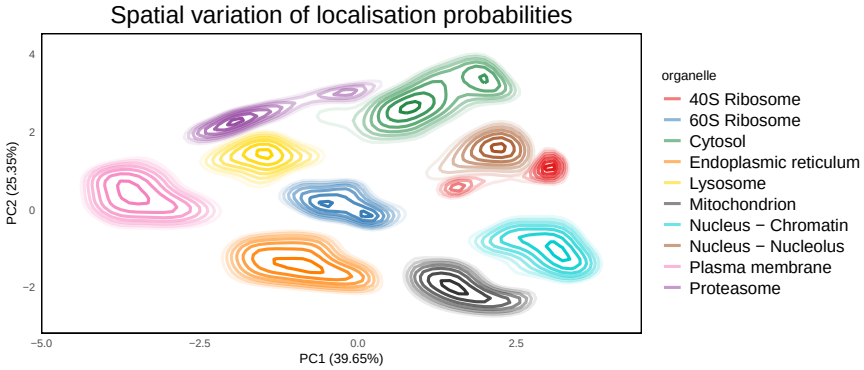

Figure 12: Visualising how the posterior localisation probabilities vary smoothly across different regions of the PCA plot. The colours correspond the different subcellular niches. The inner most contour corresponds to a probability of 0.99 and the following contour to 0.95, with each subsequent contour descreasing in 0.05 increments

```
spatial2D(object = E14TG2aR)
```

Aside from global visualisation of the data, we can also interrogate each individual protein. As illustrated on figure @ref(fig:probdists1), we can obtain the full posterior distribution of localisation probabilities for each protein from the `e14Tagm_converged_pooled` object. We can use the `plot` generic on the `MCMCParams` object to obtain a violin plot of the localisation distribution. Simply providing the name of the protein in the second argument produces the plot for that protein. The solute carrier transporter protein E9QMX3, also referred to as Slc15a1, is most probably localised to plasma membrane in line with its role as a transmembrane transporter but also shows some uncertainty, potentially also localising to other comparments. The first violin plot visualises this uncertainty. The protein Q3V1Z5 is a supposed constitute of the 40S ribosome and has poor UniProt annotation with evidence only at the transcript level. From the plot below it is clear that Q3V1Z5 is a ribosomal associated protein, but it previous localisation has only been computational inferred and here we provide experimental evidence of a ribosomal annotation. Thus, quantifying uncertainty recovers important additional annotations.

```
plot(e14Tagm_converged_pooled, "E9QMX3")
plot(e14Tagm_converged_pooled, "Q3V1Z5")
```

Discussion

The Bayesian analysis of biological data is of clear interest to many because of its ability to provide richer information about the experimental results. A fully Bayesian analysis differs from other machine learning approaches, since it can quantify the uncertainty in our inferences. Furthermore, we use a generative model to explicitly describe the data, which makes inferences more interpretable compared to the less interpretable outputs of black-box classifiers such as, for example, support vector machines (SVM).

Bayesian analysis is often characterised by its provision of a (posterior) probability distribution over the biological parameters of interest, as opposed to single point estimate of these parameters. In the case that is presented in this workflow, a Bayesian analysis "computes" a posterior probability distribution over the protein localisation probabilities. These probability distributions can then be rigorously interrogated for greater biological insight; in addition, it may allow us to ask additional questions about the data, such as whether a protein might be multi-localised.

Despite the wealth of information a Bayesian analysis can provide, the uptake amongst cell biologists is still low. This is because a Bayesian analysis presents a new set of challenges and little practical guidance exists regarding how to address these challenges. Bayesian analyses often rely on computatinally intensive approaches such as Markov-chain Monte-Carlo (MCMC) and a practical understanding of these algorithms and the interpretation of their output is a key barrier to their use. A Bayesian analysis usually consists of three broad steps: (1) Data pre-processing and algorithmic implementation, (2) assessing algorithmic convergence and (3) summarising and visualising the results. This workflow provides a set of tools to simplify these steps and provides step-by-step guidance in the context of the analysis of spatial proteomics data.

We have provided a workflow for the Bayesian analysis of spatial proteomics using the `pRoloc` and `MSnbase` software. We have demonstrated, in a step-by-step fashion, the challenges and advantages associated with taking a Bayesian approach to data analysis. We hope this workflow will help spatial proteomics practitioners to apply our methods and will motivate others to create detailed documentation for the Bayesian analysis of biological data.

Session information

Below, we provide a summary of all packages and versions used to generate this document.

```
sessionInfo()
```

```
## R version 3.5.2 (2018-12-20)
## Platform: x86_64-w64-mingw32/x64 (64-bit)
## Running under: Windows 10 x64 (build 17134)
##
## Matrix products: default
##
## locale:
## [1] LC_COLLATE=English_United Kingdom.1252
## [2] LC_CTYPE=English_United Kingdom.1252
## [3] LC_MONETARY=English_United Kingdom.1252
## [4] LC_NUMERIC=C
## [5] LC_TIME=English_United Kingdom.1252
##
```

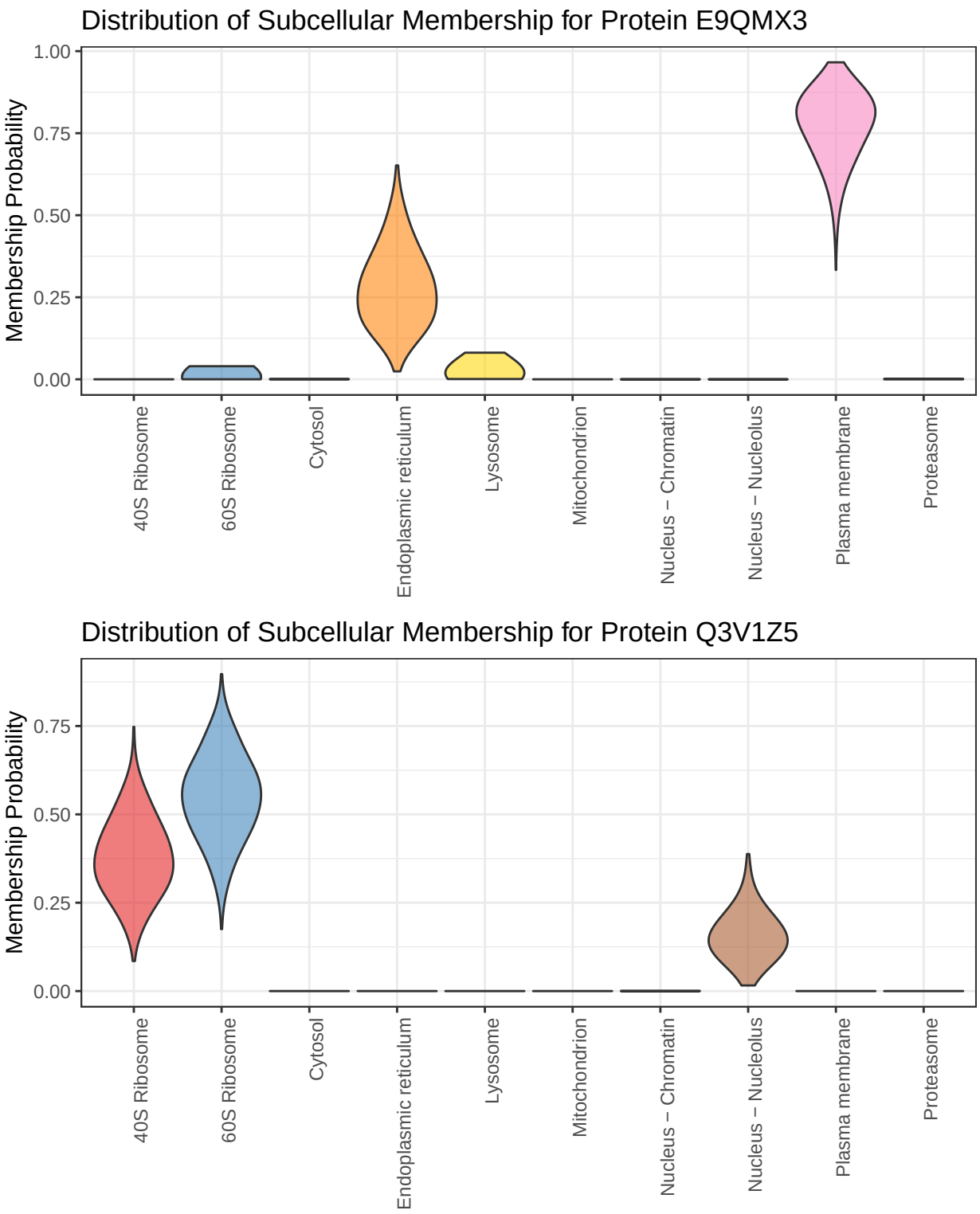

Figure 13: Full posterior distribution of localisation probabilities for individual proteins.

```
## attached base packages:
##  [1] grid      stats4    parallel  stats     graphics  grDevices utils
##  [8] datasets  methods   base
##
## other attached packages:
##  [1] patchwork_0.0.1      bindrcpp_0.2.2       pRolocdata_1.21.1
##  [4] pRoloc_1.23.2        coda_0.19-2          fields_9.6
##  [7] maps_3.3.0           spam_2.2-1           dotCall64_1.0-0
## [10] akima_0.6-2          dplyr_0.8.0.1        ggplot2_3.1.0
## [13] mixtools_1.1.0       BiocParallel_1.16.5  MLInterfaces_1.62.0
## [16] cluster_2.0.7-1      annotate_1.60.0      XML_3.98-1.17
## [19] AnnotationDbi_1.44.0 IRanges_2.16.0       MSnbase_2.8.3
## [22] ProtGenerics_1.14.0  S4Vectors_0.20.1     mzR_2.16.1
## [25] Rcpp_1.0.0           Biobase_2.42.0       BiocGenerics_0.28.0
##
## loaded via a namespace (and not attached):
##   [1] snow_0.4-3            plyr_1.8.4            igraph_1.2.4
##   [4] lazyeval_0.2.1        sp_1.3-1              splines_3.5.2
##   [7] ggvis_0.4.4           crosstalk_1.0.0       digest_0.6.18
##  [10] foreach_1.4.4         htmltools_0.3.6       viridis_0.5.1
##  [13] gdata_2.18.0          magrittr_1.5          memoise_1.1.0
##  [16] doParallel_1.0.14     sfsmisc_1.1-3         limma_3.38.3
##  [19] recipes_0.1.4         gower_0.1.2           rda_1.0.2-2.1
##  [22] lpSolve_5.6.13        prettyunits_1.0.2     colorspace_1.4-0
##  [25] blob_1.1.1            xfun_0.5              crayon_1.3.4
##  [28] RCurl_1.95-4.11       hexbin_1.27.2         genefilter_1.64.0
##  [31] bindr_0.1.1           impute_1.56.0         survival_2.43-3
##  [34] iterators_1.0.10      glue_1.3.0            gtable_0.2.0
##  [37] ipred_0.9-8           zlibbioc_1.28.0       kernlab_0.9-27
##  [40] prabclus_2.2-7        DEoptimR_1.0-8        scales_1.0.0
##  [43] vsn_3.50.0            mvtnorm_1.0-8         DBI_1.0.0
##  [46] viridisLite_0.3.0     xtable_1.8-3          progress_1.2.0
##  [49] proxy_0.4-22          bit_1.1-14            mclust_5.4.2
##  [52] preprocessCore_1.44.0 lava_1.6.5            prodlim_2018.04.18
##  [55] sampling_2.8          htmlwidgets_1.3       mcclust_1.0
##  [58] httr_1.4.0            threejs_0.3.1         FNN_1.1.3
##  [61] RColorBrewer_1.1-2    fpc_2.1-11.1          modeltools_0.2-22
##  [64] pkgconfig_2.0.2       flexmix_2.3-15        nnet_7.3-12
##  [67] caret_6.0-81          labeling_0.3          reshape2_1.4.3
##  [70] tidyselect_0.2.5      rlang_0.3.1           later_0.8.0
##  [73] munsell_0.5.0         mlbench_2.1-1         tools_3.5.2
##  [76] LaplacesDemon_16.1.1  generics_0.0.2        RSQLite_2.1.1
##  [79] pls_2.7-0             evaluate_0.13         stringr_1.4.0
##  [82] mzID_1.20.1           yaml_2.2.0            ModelMetrics_1.2.2
##  [85] knitr_1.21            bit64_0.9-7           robustbase_0.93-3
##  [88] randomForest_4.6-14   purrr_0.3.0           dendextend_1.9.0
##  [91] ncdf4_1.16            nlme_3.1-137          whisker_0.3-2
##  [94] mime_0.6              biomaRt_2.38.0        compiler_3.5.2
##  [97] rstudioapi_0.9.0      e1071_1.7-0.1         affyio_1.52.0
## [100] tibble_2.0.1          stringi_1.3.1         highr_0.7
## [103] lattice_0.20-38       trimcluster_0.1-2.1   Matrix_1.2-15
## [106] gbm_2.1.5             pillar_1.3.1          BiocManager_1.30.4
## [109] MALDIquant_1.18       data.table_1.12.0     bitops_1.0-6
## [112] httpuv_1.4.5.1        R6_2.4.0              pcaMethods_1.74.0
```

```
## [115] affy_1.60.0           hwriter_1.3.2         promises_1.0.1
## [118] gridExtra_2.3         codetools_0.2-15      MASS_7.3-51.1
## [121] gtools_3.8.1          assertthat_0.2.0      withr_2.1.2
## [124] diptest_0.75-7        hms_0.4.2             timeDate_3043.102
## [127] rpart_4.1-13          class_7.3-14          rmarkdown_1.11
## [130] segmented_0.5-3.0     lubridate_1.7.4       shiny_1.2.0
## [133] base64enc_0.1-3
```

The source of this document, including the code necessary to reproduce the analyses and figures is available in a public manuscript repository on GitHub (Crook and Gatto 2019).

Data availability

The data used in this workflow was first published in Breckels *et al.* (2016) (Breckels, Holden, et al. 2016) and is available in the pRolocdata package.

Software availability

Computational workflow for this study available from: https://github.com/ococrook/TAGMworkflow

Archived source code at time of publication: https://doi.org/10.5281/zenodo.2593712 (Oliver M. Crook et al. 2019)

License: CC BY 4.0

Grant information

PDWK was supported by the MRC (project reference MC_UU_00002/10). LMB <<<<<<< HEAD was supported by a BSRC Tools and Resources Development grant (Award BB/N023129/1) and a Wellcome Trust Technology Development Grant (Grant number 108441/Z/15/Z). OMC is a Wellcome Trust Mathematical Genomics and Medicine student supported financially by the School of Clinical Medicine, University of Cambridge. The funders had no role in study design, data collection and analysis, decision to publish, or preparation of the manuscript. ======= was supported by a BBSRC Tools and Resources Development grant (Award BB/N023129/1) and a Wellcome Trust Technology Development Grant (Grant number 108441/Z/15/Z). OMC is a Wellcome Trust Mathematical Genomics and Medicine student supported financially by the School of Clinical Medicine, University of Cambridge.

The funders had no role in study design, data collection and analysis, decision to publish, or preparation of the manuscript. >>>>>>> a294ccfa46042d30222c9a4b9655b4b00609cc48

References

Beltran, Pierre M Jean, Rommel A Mathias, and Ileana M Cristea. 2016. "A Portrait of the Human Organelle Proteome in Space and Time During Cytomegalovirus Infection." *Cell Systems* 3 (4). Elsevier: 361–73.

Betancourt, Michael. 2018. "Calibrating Model-Based Inferences and Decisions." *ArXiv Preprint ArXiv:1803.08393*.

Borg, Ingwer, and Patrick Groenen. 2003. "Modern Multidimensional Scaling: Theory and Applications."

Journal of Educational Measurement 40 (3). Wiley Online Library: 277–80.

Breckels, Lisa M, Laurent Gatto, Andy Christoforou, Arnoud J Groen, Kathryn S Lilley, and Matthew WB Trotter. 2013. "The Effect of Organelle Discovery Upon Sub-Cellular Protein Localisation." *Journal of Proteomics* 88. Elsevier: 129–40.

Breckels, Lisa M, Sean B Holden, David Wojnar, Claire M Mulvey, Andy Christoforou, Arnoud Groen, Matthew WB Trotter, Oliver Kohlbacher, Kathryn S Lilley, and Laurent Gatto. 2016. "Learning from Heterogeneous Data Sources: An Application in Spatial Proteomics." *PLoS Computational Biology* 12 (5). Public Library of Science: e1004920.

Breckels, Lisa M, Claire M Mulvey, Kathryn S Lilley, and Laurent Gatto. 2016. "A Bioconductor Workflow for Processing and Analysing Spatial Proteomics Data." *F1000Research* 5.

Brooks, Stephen P, and Andrew Gelman. 1998. "General Methods for Monitoring Convergence of Iterative Simulations." *Journal of Computational and Graphical Statistics* 7 (4). Taylor & Francis: 434–55.

Christoforou, Andy, Claire M Mulvey, Lisa M Breckels, Aikaterini Geladaki, Tracey Hurrell, Penelope C Hayward, Thomas Naake, et al. 2016. "A Draft Map of the Mouse Pluripotent Stem Cell Spatial Proteome." *Nature Communications* 7. Nature Publishing Group: 9992.

Cody, Neal AL, Carole Iampietro, and Eric Lécuyer. 2013. "The Many Functions of MRNA Localization During Normal Development and Disease: From Pillar to Post." *Wiley Interdisciplinary Reviews: Developmental Biology* 2 (6). Wiley Online Library: 781–96.

Crook, Oliver M, Kathryn S Lilley, Laurent Gatto, and Paul DW Kirk. 2019. "Semi-Supervised Non-Parametric Bayesian Modelling of Spatial Proteomics." *ArXiv Preprint ArXiv:1903.02909*.

Crook, Oliver M, Claire M Mulvey, Paul D W Kirk, Kathryn S Lilley, and Laurent Gatto. 2018. "A Bayesian Mixture Modelling Approach for Spatial Proteomics." *PLoS Comput. Biol.* 14 (11): e1006516.

Crook, Oliver M., Laurent Gatto, Paul DW Kirk, and Lisa Breckels. 2019. "Ococrook/Tagmworkflow: F1000 Submission." doi:10.5281/zenodo.2593712.

Crook, OM, and L Gatto. 2019. "A Bioconductor Workflow for the Bayesian Analysis of Spatial Proteomics." *GitHub Repository*. https://github.com/ococrook/TAGMworkflow; GitHub.

Davies, Alexandra K, Daniel N Itzhak, James R Edgar, Tara L Archuleta, Jennifer Hirst, Lauren P Jackson, Margaret S Robinson, and Georg HH Borner. 2018. "AP-4 Vesicles Contribute to Spatial Control of Autophagy via Rusc-Dependent Peripheral Delivery of Atg9a." *Nature Communications* 9. Nature Publishing Group: 3958.

De Matteis, Maria Antonietta, and Alberto Luini. 2011. "Mendelian Disorders of Membrane Trafficking." *New England Journal of Medicine* 365 (10). Mass Medical Soc: 927–38.

Dempster, Arthur P, Nan M Laird, and Donald B Rubin. 1977. "Maximum Likelihood from Incomplete Data via the Em Algorithm." *Journal of the Royal Statistical Society. Series B (Methodological)*. JSTOR, 1–38.

Dunkley, Tom PJ, Svenja Hester, Ian P Shadforth, John Runions, Thilo Weimar, Sally L Hanton, Julian L Griffin, et al. 2006. "Mapping the Arabidopsis Organelle Proteome." *Proceedings of the National Academy of Sciences* 103 (17). National Acad Sciences: 6518–23.

Dunkley, Tom PJ, Rod Watson, Julian L Griffin, Paul Dupree, and Kathryn S Lilley. 2004. "Localization of Organelle Proteins by Isotope Tagging (Lopit)." *Molecular & Cellular Proteomics* 3 (11). ASBMB: 1128–34.

Foster, Leonard J, Carmen L de Hoog, Yanling Zhang, Yong Zhang, Xiaohui Xie, Vamsi K Mootha, and Matthias Mann. 2006. "A Mammalian Organelle Map by Protein Correlation Profiling." *Cell* 125 (1). Elsevier: 187–99.

Fraley, Chris, and Adrian E Raftery. 2005. "Bayesian Regularization for Normal Mixture Estimation and Model-Based Clustering." *Techincal Report*. Washington Univ Seattle Dept of Statistics.

Gatto, Laurent, Lisa M Breckels, Thomas Burger, Daniel JH Nightingale, Arnoud J Groen, Callum Campbell,

Claire M Mulvey, Andy Christoforou, Myriam Ferro, and Kathryn S Lilley. 2014a. "A Foundation for Reliable Spatial Proteomics Data Analysis." *Molecular & Cellular Proteomics*. ASBMB, mcp–M113.

Gatto, Laurent, Lisa M. Breckels, Samuel Wieczorek, Thomas Burger, and Kathryn S. Lilley. 2014b. "Mass-Spectrometry Based Spatial Proteomics Data Analysis Using PRoloc and PRolocdata." *Bioinformatics*.

Geladaki, Aikaterini, Nina Kocevar Britovsek, Lisa M Breckels, Tom Sand Owen L Vennard Smith, Claire M Mulvey, Oliver M Crook, Laurent Gatto, and Kathryn S Lilley. 2019. "Combining Lopit with Differential Ultracentrifugation for High-Resolution Spatial Proteomics." *Nature Communications* 10. Nature Publishing Group: 331.

Gelman, A., J. B. Carlin, H. S. Stern, and D. B. Rubin. 1995. *Bayesian Data Analysis*. London: Chapman & Hall.

Gelman, Andrew, and Donald B Rubin. 1992. "Inference from Iterative Simulation Using Multiple Sequences." *Statistical Science*. JSTOR, 457–72.

Geweke, John. 1992. "Evaluating the Accuracy of Sampling-Based Approaches to the Calculation of Posterior Moments." *BAYESIAN STATISTICS*. Citeseer.

Gibson, Toby J. 2009. "Cell Regulation: Determined to Signal Discrete Cooperation." *Trends in Biochemical Sciences* 34 (10). Elsevier: 471–82.

Gilks, Walter R, Sylvia Richardson, and David Spiegelhalter. 1995. *Markov Chain Monte Carlo in Practice*. Chapman; Hall/CRC.

Gneiting, Tilmann. 2002. "Nonseparable, Stationary Covariance Functions for Space–time Data." *Journal of the American Statistical Association* 97 (458). Taylor & Francis: 590–600.

Hall, Stephanie L, Svenja Hester, Julian L Griffin, Kathryn S Lilley, and Antony P Jackson. 2009. "The Organelle Proteome of the Dt40 Lymphocyte Cell Line." *Molecular & Cellular Proteomics* 8 (6). ASBMB: 1295–1305.

Hirst, Jennifer, Daniel N Itzhak, Robin Antrobus, Georg HH Borner, and Margaret S Robinson. 2018. "Role of the Ap-5 Adaptor Protein Complex in Late Endosome-to-Golgi Retrieval." *PLoS Biology* 16 (1). Public Library of Science: e2004411.

Itzhak, Daniel N, Colin Davies, Stefka Tyanova, Archana Mishra, James Williamson, Robin Antrobus, Jürgen Cox, Michael P Weekes, and Georg HH Borner. 2017. "A Mass Spectrometry-Based Approach for Mapping Protein Subcellular Localization Reveals the Spatial Proteome of Mouse Primary Neurons." *Cell Reports* 20 (11). Elsevier: 2706–18.

Itzhak, Daniel N, Stefka Tyanova, Jürgen Cox, and Georg HH Borner. 2016. "Global, Quantitative and Dynamic Mapping of Protein Subcellular Localization." *Elife* 5. eLife Sciences Publications Limited: e16950.

Jadot, Michel, Marielle Boonen, Jaqueline Thirion, Nan Wang, Jinchuan Xing, Caifeng Zhao, Abla Tannous, et al. 2017. "Accounting for Protein Subcellular Localization: A Compartmental Map of the Rat Liver Proteome." *Molecular & Cellular Proteomics* 16 (2). ASBMB: 194–212.

Jeffery, Constance J. 2009. "Moonlighting Proteins - an Update." *Molecular BioSystems* 5 (4). Royal Society of Chemistry: 345–50.

Kau, Tweeny R, Jeffrey C Way, and Pamela A Silver. 2004. "Nuclear Transport and Cancer: From Mechanism to Intervention." *Nature Reviews Cancer* 4 (2). Nature Publishing Group: 106–17.

Latorre, Isabel J, Michael H Roh, Kristopher K Frese, Robert S Weiss, Ben Margolis, and Ronald T Javier. 2005. "Viral Oncoprotein-Induced Mislocalization of Select Pdz Proteins Disrupts Tight Junctions and Causes Polarity Defects in Epithelial Cells." *Journal of Cell Science* 118 (18). The Company of Biologists Ltd: 4283–93.

Laurila, Kirsti, and Mauno Vihinen. 2009. "Prediction of Disease-Related Mutations Affecting Protein

Localization." *BMC Genomics* 10 (1). BioMed Central: 122.

Luheshi, Leila M, Damian C Crowther, and Christopher M Dobson. 2008. "Protein Misfolding and Disease: From the Test Tube to the Organism." *Current Opinion in Chemical Biology* 12 (1). Elsevier: 25–31.

Mendes, Marta, Alberto Peláez-García, María López-Lucendo, Rubén A. Bartolomé, Eva Calviño, Rodrigo Barderas, and J. Ignacio Casal. 2017. "Mapping the Spatial Proteome of Metastatic Cells in Colorectal Cancer." *Proteomics* 17 (19). doi:10.1002/pmic.201700094.

Mulvey, Claire M, Lisa M Breckels, Aikaterini Geladaki, Nina Kočevar Britovšek, Daniel JH Nightingale, Andy Christoforou, Mohamed Elzek, Michael J Deery, Laurent Gatto, and Kathryn S Lilley. 2017. "Using hyperLOPIT to Perform High-Resolution Mapping of the Spatial Proteome." *Nature Protocols* 12 (6). Nature Research: 1110–35.

Nadaraya, Elizbar A. 1964. "On Estimating Regression." *Theory of Probability & Its Applications* 9 (1). SIAM: 141–42.

Nguyen, Lan Huong, and Susan Holmes. 2019. "Ten Quick Tips for Effective Dimensionality Reduction." *PLOS Computational Biology* 15 (6). Public Library of Science: e1006907.

Nightingale, Daniel JH, Aikaterini Geladaki, Lisa M Breckels, Stephen G Oliver, and Kathryn S Lilley. 2019. "The Subcellular Organisation of Saccharomyces Cerevisiae." *Current Opinion in Chemical Biology* 48. Elsevier: 86–95.

Olkkonen, Vesa M, and Elina Ikonen. 2006. "When Intracellular Logistics Fails-Genetic Defects in Membrane Trafficking." *Journal of Cell Science* 119 (24). The Company of Biologists Ltd: 5031–45.

Orre, Lukas Minus, Mattias Vesterlund, Yanbo Pan, Taner Arslan, Yafeng Zhu, Alejandro Fernandez Woodbridge, Oliver Frings, Erik Fredlund, and Janne Lehtiö. 2019. "SubCellBarCode: Proteome-Wide Mapping of Protein Localization and Relocalization." *Molecular Cell* 73 (1): 166–182.e7. doi:https://doi.org/10.1016/j.molcel.2018.11.035.

Plummer, Martyn, Nicky Best, Kate Cowles, and Karen Vines. 2006. "CODA: Convergence Diagnosis and Output Analysis for Mcmc." *R News* 6 (1): 7–11. https://journal.r-project.org/archive/.

Ren, Boyu, Sergio Bacallado, Stefano Favaro, Susan Holmes, and Lorenzo Trippa. 2017. "Bayesian Nonparametric Ordination for the Analysis of Microbial Communities." *Journal of the American Statistical Association* 112 (520). Taylor & Francis: 1430–42.

Roberts, Gareth O, and Adrian FM Smith. 1994. "Simple Conditions for the Convergence of the Gibbs Sampler and Metropolis-Hastings Algorithms." *Stochastic Processes and Their Applications* 49 (2). Elsevier: 207–16.

Rodriguez, José Antonio, Wendy WY Au, and Beric R Henderson. 2004. "Cytoplasmic Mislocalization of Brca1 Caused by Cancer-Associated Mutations in the Brct Domain." *Experimental Cell Research* 293 (1). Elsevier: 14–21.

Shin, Soo J, Jeffrey A Smith, Günther A Rezniczek, Sheng Pan, Ru Chen, Teresa A Brentnall, Gerhard Wiche, and Kimberly A Kelly. 2013. "Unexpected Gain of Function for the Scaffolding Protein Plectin Due to Mislocalization in Pancreatic Cancer." *Proceedings of the National Academy of Sciences* 110 (48). National Acad Sciences: 19414–9.

Siljee, J E, Y Wang, A A Bernard, B A Ersoy, S Zhang, A Marley, M Von Zastrow, J F Reiter, and C Vaisse. 2018. "Subcellular Localization of MC4R with ADCY3 at Neuronal Primary Cilia Underlies a Common Pathway for Genetic Predisposition to Obesity." *Nat Genet*, January. doi:10.1038/s41588-017-0020-9.

Smith, Adrian FM, and Gareth O Roberts. 1993. "Bayesian Computation via the Gibbs Sampler and Related Markov Chain Monte Carlo Methods." *Journal of the Royal Statistical Society. Series B (Methodological).*

JSTOR, 3–23.

Stein, Michael L. 1999. “Interpolation of Spatial Data: Some Theory for Kriging.” Springer.

Tan, Denise JL, Heidi Dvinge, Andrew Christoforou, Paul Bertone, Alfonso Martinez Arias, and Kathryn S Lilley. 2009. “Mapping Organelle Proteins and Protein Complexes in Drosophila Melanogaster.” *Journal of Proteome Research* 8 (6). ACS Publications: 2667–78.

Thul, Peter J, Lovisa Åkesson, Mikaela Wiking, Diana Mahdessian, Aikaterini Geladaki, Hammou Ait Blal, Tove Alm, et al. 2017. “A Subcellular Map of the Human Proteome.” *Science* 356 (6340). American Association for the Advancement of Science: eaal3321.

Vats, Dootika, and Christina Knudson. 2018. “Revisiting the Gelman-Rubin Diagnostic.” *ArXiv Preprint ArXiv:1812.09384*.

Vehtari, Aki, Andrew Gelman, Daniel Simpson, Bob Carpenter, and Paul-Christian Bürkner. 2019. “Rank-Normalization, Folding, and Localization: An Improved *widehat{R}*for Assessing Convergence of Mcmc.” *ArXiv Preprint ArXiv:1903.08008*.

Watson, Geoffrey S. 1964. “Smooth Regression Analysis.” *Sankhyā: The Indian Journal of Statistics, Series A*. JSTOR, 359–72.

Wendland, Holger. 1995. “Piecewise Polynomial, Positive Definite and Compactly Supported Radial Functions of Minimal Degree.” *Advances in Computational Mathematics* 4 (1). Springer: 389–96.